JOC The Journal of Organic Chemistry

ARTICLE

pubs.acs.org/joc

Synthesis, Spectroscopic Properties, and Electropolymerization of Azulene Dyads

Gilbert Nöll,*[,†] Jörg Daub,[‡] Michaela Lutz,[‡] and Knut Rurack*[,§]

[†]FB 8, Organische Chemie, Universität Siegen, Adolf Reichwein Strasse 2, D-57068 Siegen, Germany

[‡]Institut für Organische Chemie, Universität Regensburg, Universitätsstrasse 31, D-93053 Regensburg, Germany

[§]Div. 1.5, BAM Bundesanstalt für Materialforschung und -prüfung, Richard-Willstätter-Str. 11, D-12489 Berlin, Germany

Supporting Information

ABSTRACT: Four azulene dyads have been synthesized and studied by spectroscopic and electrochemical methods. A triarylamine, a boron-dipyrromethene (BDP or BODIPY), a porphyrin, and an isoalloxazine moiety have been linked to an extended π electron system at the 2-position of azulene, leading to the dyads **1**−**4**, respectively. For the synthesis of **1**−**4**, first 2-(4-ethynylphenyl)azulene (EPA) was prepared, which was further reacted with the halogenated chromophores by Pd-catalyzed cross-coupling reactions. The dyads **1**−**4** exhibit strong absorption bands in the visible range, which are dominated by the absorption spectra of the individual subchromophores. Fluorometric studies of **2**−**4** revealed that after excitation of the subchromophoric unit attached to the parent azulene moiety, quenching mainly through energy transfer to azulene is effective, whereas possible charge-transfer interactions play only a minor role. Potentiodynamic oxidation of the dyads **1**−**4** leads to the formation of polymer films, which are deposited at the electrode. The polymer film derived from **1** was further characterized by spectroelectrochemistry. During positive doping of poly-**1**, a strong absorption band appears at 13,200 cm^{-1}, which is typical for triarylamine radical cations. This band is overlapping with a broad absorption band in the low-energy region that might be caused by charge-transfer interactions within the polymer.

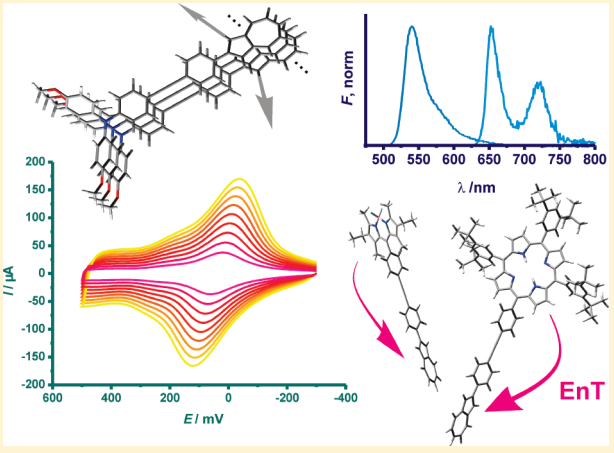

INTRODUCTION

Organic π-conjugated materials from the monomer up to the polymer level are of great interest for applications in molecular electronics or the development of organic photovoltaic (OPV) devices.[1−15] In contrast to systems based on thiophene or phenylene vinylene subunits,[6−8] only few studies have been carried out on azulene derivatives with respect to applications in OPV devices up to now.[16−32] Recently, 3-(azulen-1-yl)-2-cyanoacrylic acid, 5-(azulen-1-yl)-2-cyanopenta-2,4-dienoic acid, and derivatives have been studied as sensitizers in dye-sensitized solar cells (DSSCs).[20] These dyes exhibit a strong absorption band caused by a $S_2 \leftarrow S_0$ transition and a weak absorption due to a $S_1 \leftarrow S_0$ transition in the visible spectral range. From the experimental results it was concluded that, besides electron injection from the S_1 state, direct electron injection from the S_2 state to the TiO_2 conduction band is possible.[20] In addition, polyazulenes, which can be synthesized by chemical[16,33] and electrochemical methods,[16,34−43] have been suggested for applications in OPV devices.[16] In a previous work, we have studied the structure and electronic properties of 1,3-poly- and oligoazulenes.[16] These materials exhibit a broad absorption band (HOMO−LUMO-based $S_1 \leftarrow S_0$ transition), which covers the range between 400 and 850 nm, in which the solar irradiation spectrum has its highest intensity. Even though the molar absorption coefficient across the low-energy absorption band of azulene is rather low, azulene derivatives as such represent small and tightly packed units with a small HOMO−LUMO gap already in their monomer form. This is a significant advantage compared to transparent thiophene or phenylene vinylene building blocks for oligomers or polymers, which are frequently used in OPV devices.[6−8] In addition, the optical and electronic properties of azulene can be further tuned in a facile manner, for instance, by attachment of additional (electron-rich or electron-poor) chromophoric groups to the parent core.

To study the electronic interaction between azulene and such chromophoric groups with selected electronic and optical properties, the azulene dyads **1**−**4** were synthesized (Chart 1).[44] In **1**, a redox-active dianisylphenylamine moiety was introduced because such electron-rich triarylamine derivatives exhibit high charge

Received: January 13, 2011
Published: April 20, 2011

   dx.doi.org/10.1021/jo200080v | J. Org. Chem. 2011, 76, 4859–4873

Chart 1. Chemical Structures of the Azulene Dyads 1−4[a]

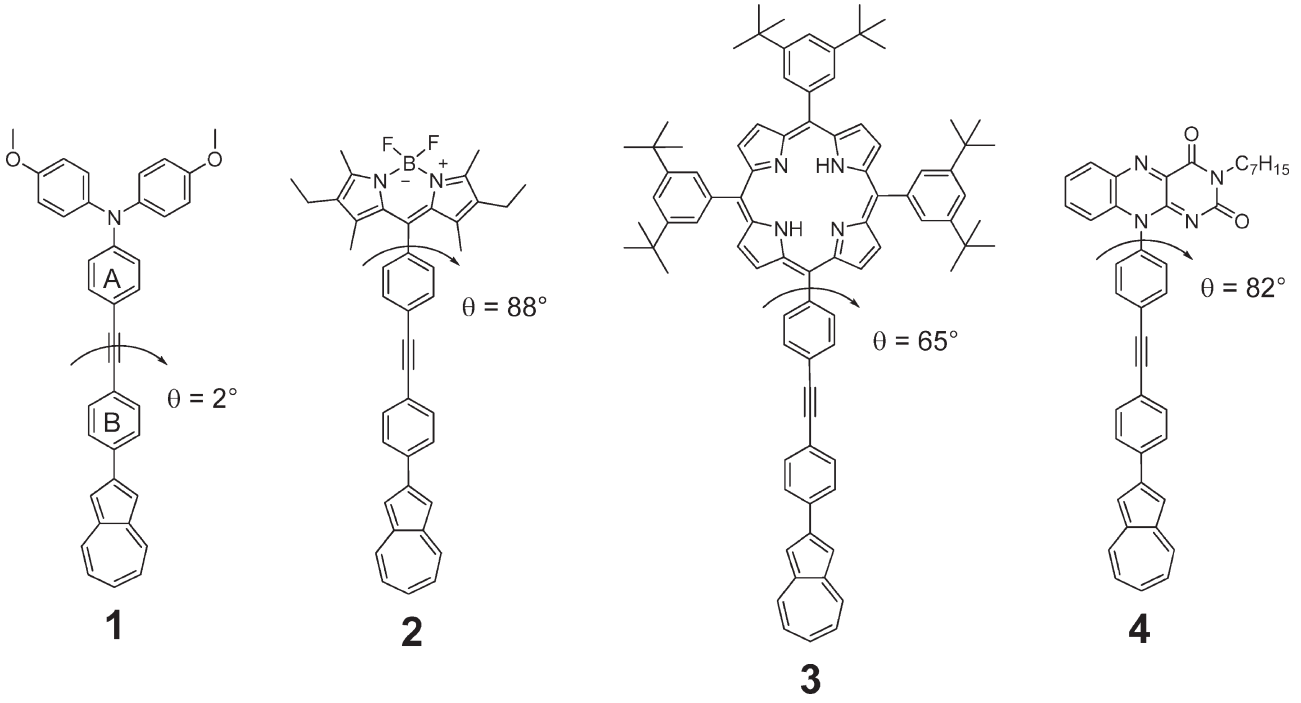

[a]Triarylamine, boron dipyrromethene, porphyrin, and isoalloxazine were chosen as functional units. Dihedral angles θ for intramolecular twisting between the azulene and the different appended chromophore units are indicated. For **1**, θ describes the angle between the planes of the two phenyl rings attached to the ethynyl spacer (labeled A, B). This angle is rather similar in all the compounds, varying between 1.5° and 2.5°.

carrier mobilities, which is of utmost importance for applications in OPV devices.[45,46] Triarylamines are widely used as hole carrier materials in optoelectronic devices, photorefractive materials, photoconductors, organic light emitting diodes and photovoltaic cells.[47−53] In dyad **2**, a boron-dipyrromethene (BDP or BODIPY) dye was used because many BDP dyes absorb intensely in the visible spectral range and exhibit high fluorescence quantum yields. BDPs have been used for several analytical applications such as proton[54,55] or metal ion[56−58] indication, as photosensitizers,[59−61] and in molecular switches.[62−65] Furthermore, the BDP subunit was employed in solar concentrators,[66−68] photonic wires,[69−71] and artificial photosynthetic antenna-reaction center assemblies.[72−74] The azulene-porphyrin dyad **3** was synthesized because porphyrins have been employed as electron donors in several dyads and triads for photoinduced electron transfer (ET) reactions, which may result in charge separation over large distances as required for photovoltaic applications.[72,75,76] In contrast to other azulene-porphyrin dyads, which have been studied previously,[77−80] in **3** both dyes are linked by an extended π electron system. Dyad **4** was prepared because flavins are the active unit of many blue-light photoreceptors[81−84] and usually act as strong electron acceptors, potentially generating charge-separated states.

Besides their synthesis, the main interest of the work reported herein was to study the interaction between azulene and the attached chromophores in the monomeric compounds. However, with azulene as the core component, polymerization at the 1/3 position of the azulene subunits in **1**−**4** should also be possible. For **4**, this would result in the formation of a double-cable polymer.[1,85,86] Intrinsically ambipolar materials are an interesting alternative to blends of an electron donating polymer with electron acceptors for applications in OPV devices of the bulk heterojunction type, because when the acceptor units are linked covalently to the electron-donating polymer, phase separation is prevented.[1,85,86] Thus, preliminary electrochemical polymerization studies complement the research described in this contribution.

RESULTS AND DISCUSSION

Synthesis. Our first goal was the preparation of 2-(4-ethynylphenyl)azulene (EPA), which can be linked to several halogenated dyes by Pd-catalyzed cross-coupling reactions. This afforded the synthesis of the photochromic 2-(4-iodophenyl)-dihydroazulene (2-(4-iodophenyl)-DHA)[87,88] as an intermediate, which converts into the corresponding vinylheptafulvene (VHF) under illumination (Scheme S-1, Supporting Information). Elimination of HCN from 2-(4-iodophenyl)-DHA in the dark led to 2-(4-iodophenyl)-azulene-1-carbonitrile, which was further reacted to 2-(4-iodophenyl)-azulene by hydrolysis of the CN-substituent followed by CO_2 evaporation.[89] EPA was obtained by a Sonogashira−Hagihara cross-coupling reaction of 2-(4-iodophenyl)-azulene with trimethylsilylacetylene and subsequent deprotection of the ethynylene group. The synthetic route is depicted in Scheme 1. For other syntheses of azulenes via DHA, see refs 39−41 and 90−92. As depicted in Scheme 2, EPA was further coupled with the halogenated chromophores **1a**−**4a**, resulting in the formation of **1**−**4**. *N*,*N*-Di(4-methoxyphenyl)-4-iodo-phenylamine **1a** was prepared according to ref 93, **2a** and **3a** through routes adapted from refs 94−96, and the synthesis of **4a** is described in the Experimental Section.

Optical Spectroscopic Investigations. The absorption spectra of **1**−**4** in CH_2Cl_2 in comparison to neat azulene are shown in Figure 1. As would be expected, the characteristic absorption

dx.doi.org/10.1021/jo200080v |J. Org. Chem. 2011, 76, 4859–4873

Scheme 1. Synthesis of 2-(4-Ethynyl-phenyl)azulene (EPA) from 2-(4-Iodophenyl)-dihydroazulene (DHA)[a]

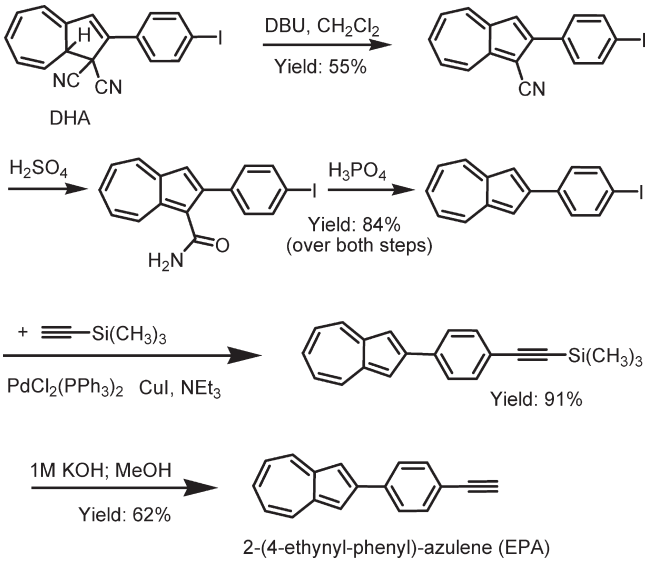

[a] For the synthesis of DHA, see Scheme S-1 in Supporting Information.

bands of the chromophore subunits dominate the spectra of **1**−**4** in the near-UV and visible spectral range. However, with the example of **2**, Figure 2 reveals that the characteristic low-energy absorption band of azulene is preserved. Interestingly, this is observed for all of the dyads, that is, irrespective of the degree of decoupling between the azulene π system and the π system of the attached chromophore unit (for dihedral angles of the geometry-optimized structures in the gas phase, see Chart 1). This is consistent with the finding that the azulene-centered low-energy transition is also preserved in EPA, in which the phenyl ring and the azulene ring system are twisted by only 23°; see Figures 2 and 3.

To get a better understanding of the photophysical processes operative in the dyads, the absorption and steady-state and time-resolved fluorescence features of **1**−**4** and EPA were investigated in solvents of different polarity at room temperature and at 77 K. Because of a partly limited solubility of the dyads, acetonitrile (MeCN, ε_r = 35.94, n_D = 1.344), tetrahydrofuran (THF, ε_r = 7.58, n_D = 1.407), and di-*n*-butylether (Bu_2O, ε_r = 3.08, n_D = 1.399) were employed in these studies; 2-methyl-THF (2-MTHF) had to be used for the low-temperature glasses.

Spectroscopic Properties of EPA. Before we discuss the properties of the dyads in more detail, it is helpful to rationalize the impact of phenylethynyl elongation in EPA compared with azulene. Figure 3 shows the respective absorption spectra in MeCN. Apparently, such an elongation of the chromophoric π system of azulene only leads to a bathochromic shift of the higher-energy transitions, for instance, from ca. 335 to 385 nm for the center of the S_2 transition. The inset, which is similar to the top right graph in Figure 2, only recorded at higher concentrations, supports the above statement that the oscillator-weak azulene-localized transitions are only barely affected. With respect to the fluorescence properties, EPA shows the typical azulene characteristics of a weak fluorescence from the S_2 state (Figure 4). As would be expected for a molecule with a small ground-state dipole moment and the lack of explicit electron-rich and electron-poor substituents such as EPA, the fluorescence maximum at ca. 405 nm does not shift significantly with solvent polarity (Table 1). In addition, the fluorescence deactivation features are also barely affected by the solvent, and the fluorescence quantum yields Φ_f of EPA amount to ca. 1×10^{-3} (Table 1). Although these values are much smaller than the fluorescence quantum yields of azulene, e.g., 0.041,[97] 0.040,[98] and 0.046[98] in ethanol, MeCN, and cyclohexane, respectively, they are comparable to Φ_f of other π extended azulenes such as **6** (e.g., $\Phi_f = 9.5 \times 10^{-4}$ in cyclohexane [CH]) or **7** (e.g., $\Phi_f = 1.3 \times 10^{-3}$ in CH; for chemical structures, see Chart 2),[99] despite the fact that the S_2-S_1 energy gap $\Delta E(S_2-S_1)$ = 10400 cm^{-1} in EPA is much smaller than $\Delta E(S_2-S_1)$ = 12,200 cm^{-1} of **6** and 12,300 cm^{-1} of **7**, both in cyclohexane.[99] For comparison, $\Delta E(S_2-S_1)$ = 13,950 cm^{-1} for azulene in MeCN.[98] Apparently, our results on EPA stress the findings of earlier studies on alkylated and halogenated azulenes that the energy gap rule is not the only decisive parameter in controlling the yield of S_2 emission in azulenes.[98,100] For instance, an alkylated azulene derivative such as **8** (Chart 2) shows intermediate $\Delta E(S_2-S_1)$, e.g., 11,840 cm^{-1} in CH_2Cl_2, yet the quantum yields are generally lower than those of EPA, **6** and **7**, e.g., $\Phi_f = 4 \times 10^{-4}$ in CH_2Cl_2.[98] However, due to the sparse number of studies on π extended azulenes and the many open mechanistic questions on simpler substituted azulenes, we cannot interpret our results in closer context of the data available from the literature. With respect to excited S_2 state relaxation, our fluorescence lifetime data on azulene (1.15 ns in MeCN, 1.13 ns in Bu_2O) agree well with the published data (e.g., 1.17 ns in CH_2Cl_2).[98] The corresponding data for EPA are again virtually solvent-independent and in the lower picosecond range (Table 1).

Spectroscopic Behavior of 1. Returning to the spectral features of the dyads, Figure 5 shows that the absorption spectra of **1** are negligibly influenced by solvent polarity, the slight shifts in the band maxima correlating with the refractive index of the solvent (vide supra) and thus being mostly due to dispersive interactions. Above 500 nm, only the typical bands localized on the azulene fragment are found (Figure 5, inset). In accordance with the spectroscopic behavior of several substituted dianisylphenylamine model compounds (Chart 3), the intense band at ca. 415 nm is attributed to a charge-transfer (CT) transition involving triarylamine donor and the ethynyl-appended moiety as acceptor. For instance, the absorption spectra of **9** are also solvent-independent with maxima of the CT bands at ca. 420 nm.[101] Since **9** is as planar as **1**, the CT bands of both **1** and **9** are comparably intense with molar absorption coefficients >20,000 M^{-1} cm^{-1}. As would be expected, the azulene-triarylamine dyad **10**, lacking a phenyl group in the π system with respect to **1**, shows a somewhat hypsochromically shifted CT band of comparable intensity at ca. 410 nm.[102] In addition, if polycyclic aromatic groups are directly attached to the phenyl ring of the dianisylphenylamine moiety as in **11**, a steric distortion of the π conjugated system is induced and the intensity of the CT band is found in a similar wavelength range yet is markedly reduced (e.g., ε_{406} = 6830 M^{-1} cm^{-1} in CH_2Cl_2).[103] The intense band in the 300−350 nm region is attributed to overlapping transitions localized on the EPA fragment (see Figure 3) and triarylamine-localized transitions; for comparison, triphenylamine shows an intense band (e.g., ε_{300} = 23,700 M^{-1} cm^{-1} in cyclohexane) at ca. 300 nm.[104] Although **1** thus is a CT-active dyad like the models shown in Chart 3, in contrast to **9**−**11** and in accordance with other donor−acceptor dyes integrating azulene,[105] it is nonfluorescent ($\Phi_f < 10^{-5}$) in the three solvents investigated.

dx.doi.org/10.1021/jo200080v |J. Org. Chem. 2011, 76, 4859–4873

Scheme 2. Synthesis of Azulene Dyads 1−4 Employing Sonogashira−Hagihara Cross-Coupling Reactions between EPA and the Corresponding Halogenated Chromophores 1a−4a

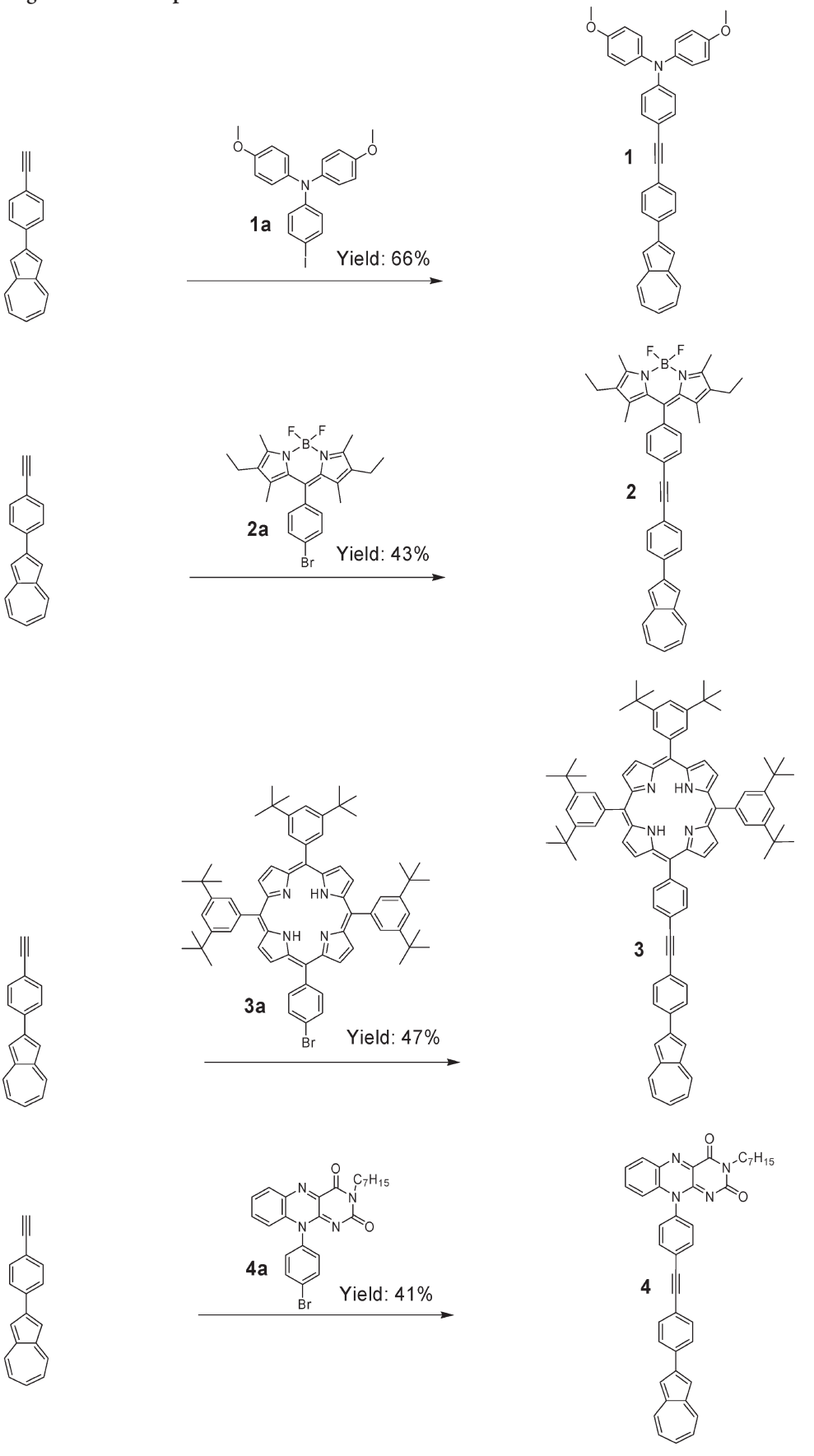

dx.doi.org/10.1021/jo200080v |J. Org. Chem. 2011, 76, 4859–4873

Spectroscopic Behavior of 2. In contrast to **1**, the two subchromophores in **2** are virtually perpendicular, preventing direct π conjugation and rendering the occurrence of CT absorption bands rather unlikely. Indeed, a comparison of the spectra in Figures 2 and 3 suggests that the bands of **2** centered at ca. 320 and 395 nm reflect the overlap of transitions located on the BDP and the π extended azulene fragment. Apparently, the orthogonal twisting of **2** divides the compound formally into a BDP and an azulene-phenyl-ethynyl-phenyl chromophore, and the entire absorption spectrum of **2** is thus a linear combination of the spectra of the two subchomophores.[106]

The results of the fluorescence studies of **2** are collected in Table 2, and representative fluorescence excitation and emission spectra are shown in Figures 2 and 4. It is apparent that only the characteristic emission band of the BDP moiety is found at its designated position (Figure 4, Table 2). Moreover, the fluorescence excitation spectrum corresponds to the typical absorption spectrum of the isolated parent BDP chromophore (Figure 2). Charge-transfer type interactions with radiative or nonradiative charge recombination thus do not play a major role for dyad **2**. A comparison of the fluorescence quantum yields and lifetimes listed in Table 2 further suggests that an increase in solvent polarity does not lead to a pronounced acceleration of a quenching process. The slight increase of Φ_f and τ_f from 0.094 to 0.118 and 0.53 to 0.60 ns upon going from MeCN to Bu_2O renders the population of such a nonemissive state by a photoinduced electron transfer process only a minor pathway. However, a comparison of Φ_f of **2** with that of its parent compound **12** (Chart 3, $\Phi_f = 0.87$ in MeCN)[63] shows that the fluorescence is quenched by a factor of ca. 20 in the case of **2**. In view of the position of the fluorescence band of the heteroaromatic chromophore in the 500−700 nm region and the weak absorption band of the azulene-based polymerizable unit between 450 and 700 nm, this quenching is tentatively ascribed to energy transfer from the excited BDP to the azulene fragment.

When we analyze the data of **2** in terms of an intramolecular Förster resonance energy transfer (FRET) process,[107] we arrive at a spectral overlap integral $J = 3.1 \times 10^{13}$ M^{-1} cm^{-1} according to eq 1. Together with the geometry factor $\kappa^2 = 2/3$ for random orientation of the two subunits, the fluorescence quantum yield of the unperturbed donor ($\Phi_D = 0.87$ for **12** in MeCN) and the refractive index n of the solvent, an effective interaction radius $R_0 = 28$ Å is obtained with eq 2. If we further consider eqs 3 and 4, with r being the distance between the FRET partners, τ_D the lifetime of the unperturbed donor **12** (5.25 ns in CH_2Cl_2),[63] and

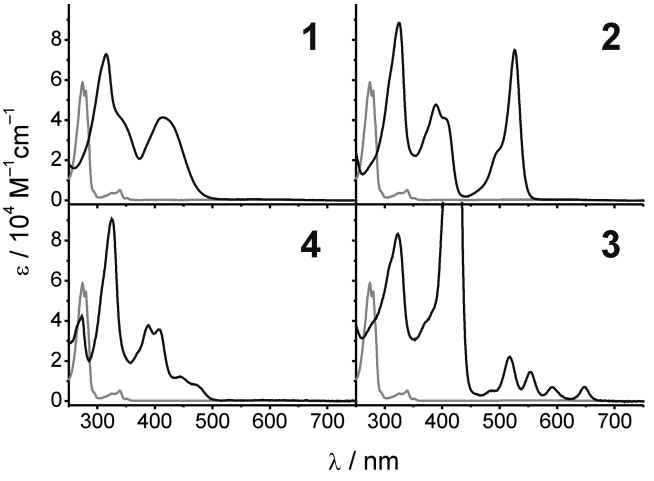

Figure 1. Absorption spectra of **1**−**4** in CH_2Cl_2 at 298 K (clockwise from top left). The spectrum of neat azulene (gray) is included for comparison. The Soret band of **3** (λ_{max} = 422 nm, ε = 590,000 M^{-1} cm^{-1}) is truncated for better comparison.

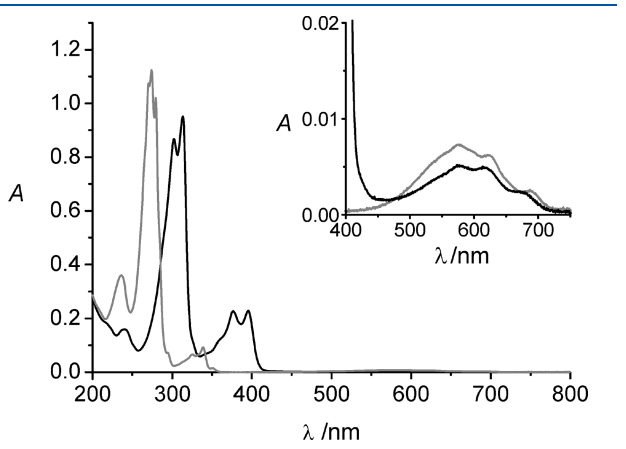

Figure 3. Absorption spectra of EPA (black) and azulene (gray) in MeCN at 298 K. The inset shows an enlargement of the 400−750 nm region.

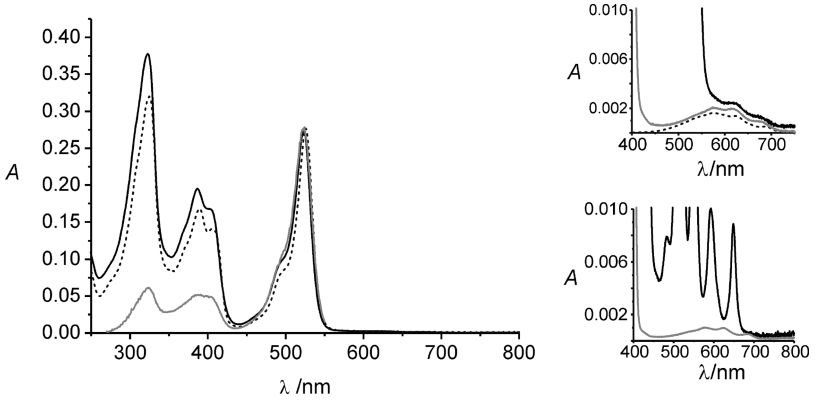

Figure 2. (Left) Absorption spectra of **2** in MeCN (solid black) and Bu_2O (dotted black) at 298 K. The corrected fluorescence excitation spectrum of **2** in MeCN (gray) is included for comparison (see text). (Right) Top: Enlargement of the 400−750 nm region with the spectra of **2** (solid black), EPA (gray) and azulene (dotted black) in MeCN. Bottom: Enlargement of the 400−800 nm region with the spectra of **3** (black) and EPA (gray) in Bu_2O.

dx.doi.org/10.1021/jo200080v |J. Org. Chem. 2011, 76, 4859–4873

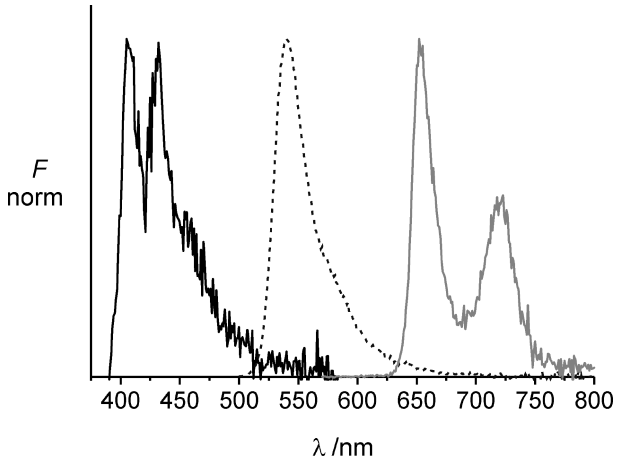

Figure 4. Normalized fluorescence spectra of **2** (dotted black), **3** (gray), and EPA (solid black) in MeCN at 298 K.

Table 1. Fluorescence Properties of EPA at Room Temperature

solvent	λ_{abs} (nm)[a]	λ_{em} (nm)	Φ_f	τ_f (ps)
MeCN	313, 395, 579 (670)	408	9×10^{-4}	13
THF	316, 399, 582 (673)	407	1×10^{-3}	17
Bu_2O	315, 399, 582 (673)	404	1×10^{-3}	17

[a] Maxima of the respective bands; for the longest-wavelength bands, the position of the lowest-energy sub-band is given in brackets.

τ_{DA} the lifetime of dyad **2**, and if we assume that no other processes contribute significantly to the deactivation of the excited BDP state, the donor−acceptor distance of the FRET partners is determined to ca. 19.5 Å, equaling within ±0.2 Å the distance between the BDP core and the center of the azulene unit as obtained from the optimized ground state geometry by DFT calculations.

$$J = \int F_D(\lambda)\varepsilon_A(\lambda)\lambda^4 d\lambda \quad (1)$$

$$R_0{}^6 = 8.875 \times 10^{-5}\frac{\kappa^2 \Phi_D J}{n^4} \quad (2)$$

$$k_{FRET} = \frac{1}{\tau_D}\left(\frac{R_0}{r}\right)^6 \quad (3)$$

$$k_{FRET} = \frac{1}{\tau_{DA}} - \frac{1}{\tau_D} \quad (4)$$

Comparative fluorescence measurements carried out at 298 and 77 K for **2** and **12** as a reference compound support this interpretation, that is, the fluorescence of **2** is still a factor of 15 smaller than that of the unperturbed BDP chromophore at low temperatures. The major intramolecular deactivation pathway is tentatively ascribed to energy transfer.

Spectroscopic Behavior of 3. For **3**, a closer inspection of the absorption spectra of **3a** (for chemical structure, see Scheme 2) and **3** reveals also a linear combination of the single spectra of the subchromophores, that is, of the porphyrin and the azulene-phenyl-ethynyl-phenyl fragments. However, as is evident from

Chart 2. Azulene Derivatives from the Literature Discussed in the Text

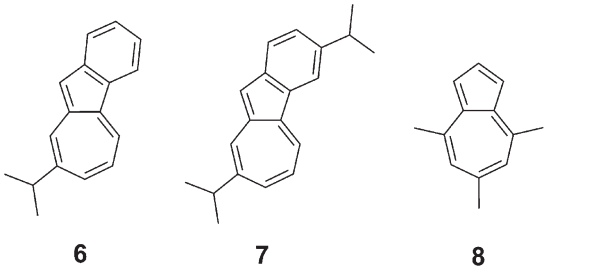

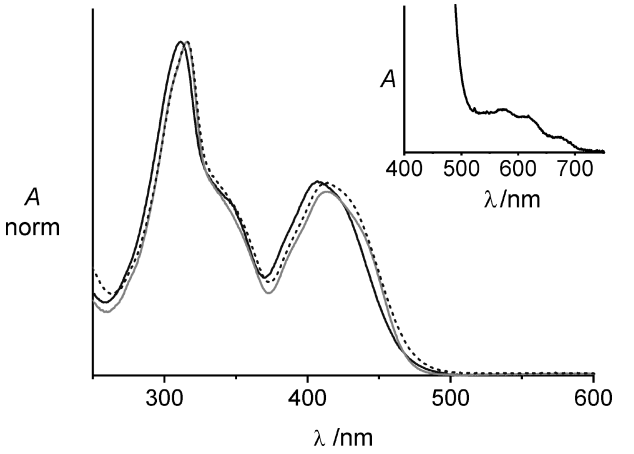

Figure 5. Absorption spectra of **1** in MeCN (black), THF (dotted), and Bu_2O (gray) at 298 K. The inset shows a representative enlargement of the 400−750 nm region with the example of MeCN.

Figure 2 and a comparison of the spectra of **3** and EPA in Figures 1 and 3, the overlap is much stronger for this dyad. Again, as for **2**, only the characteristic emission band of the porphyrin moiety is found at 654 ± 1 nm, independent of solvent polarity (Figure 4).[108] The fluorescence quantum yields and lifetimes of **3**, equaling for instance 0.01 and 1.41 ns in Bu_2O, show also no pronounced trend as a function of solvent polarity, as in the case of **2**. Moreover, also for **3** with respect to parent **13** (Chart 3, Φ_f = 0.11 in dichloroethane),[109] the fluorescence is quenched yet not as pronounced as in the BDP case. Since we did not find any hints of cyclic energy transfer as reported for an azulene-zinc porphyrin dyad in ref 78, presumably due to the distinctly weaker S_2 fluorescence of EPA (or, more precisely, the azulene-phenyl-ethynyl-phenyl fragment) compared with azulene, we analyzed the energy transfer in **3** according to the same formalism as above and obtained an effective interaction radius R_0 of ca. 19 Å and a donor−acceptor distance of ca. 16 Å.[110]

Spectroscopic Behavior of 4. For **4**, the situation with regard to spectral overlap between the absorption and emission bands is even worse than for the other two dyads. The $S_2 \leftarrow S_0$ absorption band of the azulene-phenyl-ethynyl-phenyl unit and the $S_1 \leftarrow S_0$ absorption band of the isoalloxazine moiety show pronounced overlap as does the fluorescence band of the isoalloxazine group, with a maximum at ca. 530 nm and a full width at half height of ca. 100 nm, with the low-energy absorption band of the azulene unit. Consequently, fluorescence quenching is even more efficient in this case, and the fluorescence quantum yield of flavin, determined

dx.doi.org/10.1021/jo200080v |J. Org. Chem. 2011, 76, 4859–4873

Chart 3. Dianisylphenylamine, BDP, and Porphyrin Model Compounds from the Literature Discussed in the Text[a]

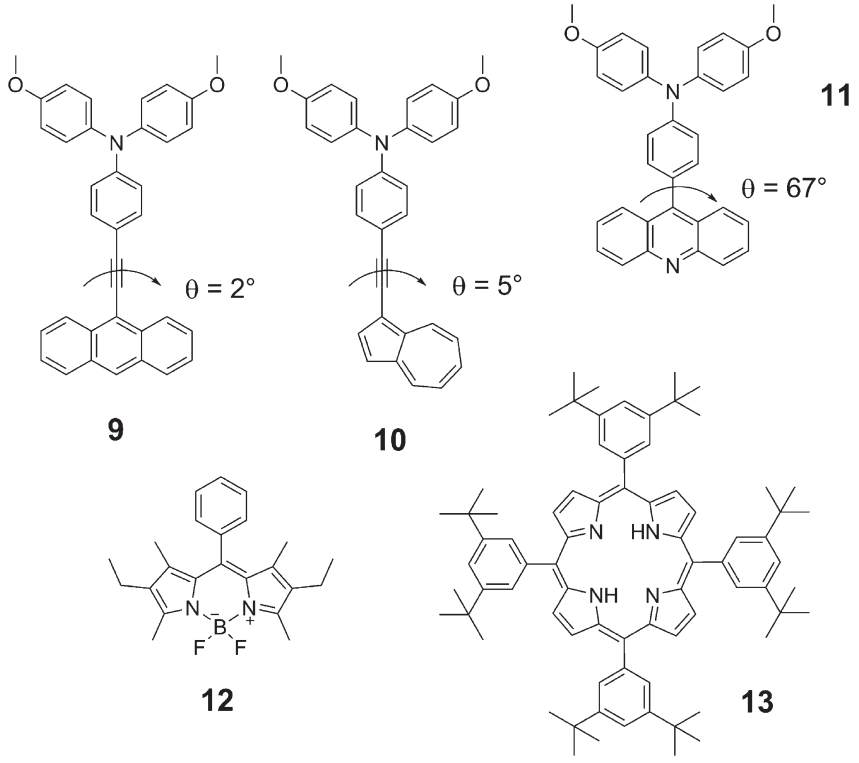

[a]For the definition of the dihedral angles θ, see the footnote of Chart 1. Angles for **9** and **10** pertain to the angle between the phenyl and anthryl or azulenyl moieties, and the angle for **11** to the twisting between the adjacent phenyl and acridinyl group.

Table 2. Fluorescence Properties of 2 at Room Temperature[a]

solvent	λ_{em} (nm)	Φ_f	τ_f (ns)
MeCN	538	0.094	0.53
THF	541	0.107	0.57
Bu_2O	539	0.118	0.60

[a] It should be noted that any possible residual fluorescence of the azulene-phenyl-ethynyl-phenyl fragment upon excitation of **2** at 375 nm could not be reliably detected, presumably due to the comparatively low quantum yield of the S_2-S_0 emission and the intense absorption of the BDP chromophores at ca. 450 nm.

to 0.16 in THF and 0.24 in MeCN by us here, is drastically reduced to ca. 1×10^{-3} for **4** in both solvents.[111] The fluorescence lifetimes of the dyad were determined to 56 and 64 ps in MeCN and THF, almost 2 orders of magnitude faster as those of flavin, 3.72 ns in THF and 4.92 ns in MeCN. Because of the strong variation of the fluorescence yield and lifetime properties of the parent compound in the two solvents employed here—the spectral band position remains almost unchanged, however—a further analysis of an energy transfer process was not attempted.

While the triarylamine moiety was attached to the azulene backbone mainly because of its ability to serve as efficient hole carrying subunit (referring to **1**), the chromophoric groups attached to the azulene core in **2**−**4** have been chosen in order to increase the absorption of light in the visible range. For a photovoltaic application, the absorption of light that is the excitation of the chromophore should lead to the formation of a charge-separated state. Apparently, this is not the case for dyads **2**−**4**, at least not in their monomeric state. However, oxidation of the azulene subunit may result in the formation of 1,3-polyazulene derivatives, and the optic and electronic properties of poly-**1**−**4** may differ significantly from those of **1**−**4** in their monomeric state. In principle, polymers of **1**−**4** can be formed by chemical or electrochemical polymerization, and depending on the polymerization conditions, polymers of different average chain length should be obtained, with mixed polymers being even possible. Since the preparation of different types of polymers and their detailed characterization would go far beyond the scope of this publication, we report here only the studies of the electrochemical behavior of dyads **1**−**4**, to gain insight about the possibility of the electrochemical formation of the corresponding polyazulene derivatives in a future step.

Electrochemical Investigations. Electrochemical Polymerization of 1. Cyclic voltammetry was performed in order to determine the oxidation potentials of **1**−**4**. The multicycle cyclic voltammograms (CVs) of **1**, collected at a scan rate of $\nu = 50$ mV s^{-1}, are depicted in Figure 6 (inset: initial cycle with $\nu = 250$ mV s^{-1}). The potentiodynamic oxidation of **1** leads to polymerization, which results in the formation of polymer films at the electrode. During this process, two major oxidative waves are present ($E_{1/2}$ at ca. 270 and 900 mV vs Fc/Fc^+). By comparison with related azulene-triarylamine systems, the first wave (at less positive potentials) is assigned to the oxidation of the triarylamine subunit (almost reversible at fast scan rates) and the second to the irreversible oxidation of the azulene moiety.[16] This assignment is supported by the fact that redox potentials of $E_{1/2} = 109$ mV vs Fc/Fc^+ and $E_{1/2} = 600$ mV vs Fc/Fc^+ have been reported for trianisylamine[112] and azulene in CH_2Cl_2.[16]

dx.doi.org/10.1021/jo200080v |J. Org. Chem. 2011, 76, 4859–4873

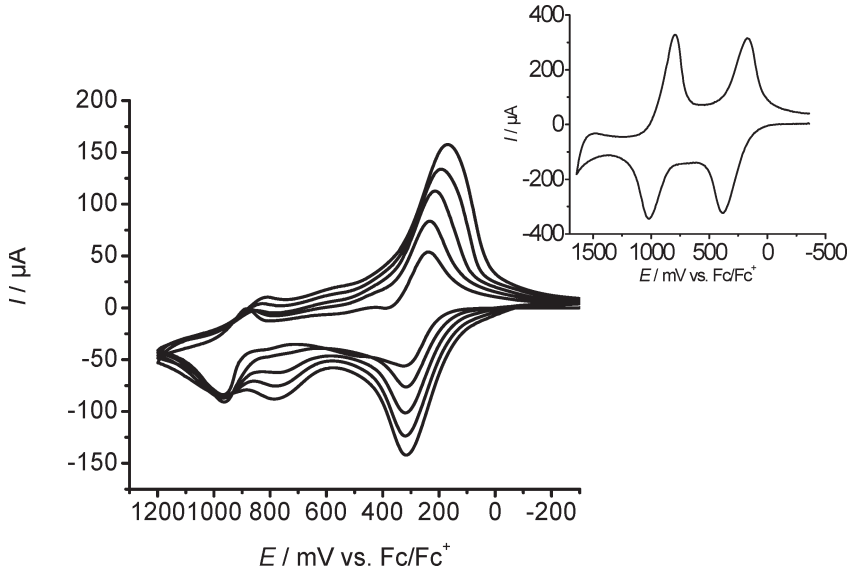

Figure 6. Multicycle CVs (5 cycles) showing the potentiodynamic oxidative polymerization of **1** in CH_2Cl_2 at a scan rate of $\nu = 50$ mV s^{-1} (inset: initial cycle measured at $\nu = 250$ mV s^{-1}).

When multicycle CVs at low scan rates were performed only on the first oxidation of **1**, electrochemical polymerization was observed as well (Figure S-1, Supporting Information). Obviously, the oxidation of the triarylamine is followed by ET from the azulene resulting in subsequent polymerization. Hence, there is a strong electronic coupling in the azulene-triarylamine dyad.

The multicycle CVs of the resulting polymer film in monomer-free solution (Figure 7A) are dominated by one single oxidative wave, which is assigned to the reduction of the triarylamine redox moiety in the polymer. Hence, the electrochemical properties of films of **1** are dominated by the triarylamine subunit at low to moderately positive potentials. The polymer films were highly stable in the depicted potential range. When the potential was increased to more positive values, the polymer films showed some decrease with each cycle. An analogous behavior has been reported for polyazulene at high doping levels.[16] The CVs of the polymer film of **1** in monomer-free solution at different scan rates (Figure 7B) exhibit a linear increase of the current with scan rate, as is expected for a process without limiting diffusion.

Electrochemical Polymerization of 2. Compound **2** could be polymerized upon electrochemical polymerization as well (Figure S-2). Again, two oxidative subwaves were found. However, this time the first wave was not reversible at all (Figure S-2, inset a). Since both the oxidation of azulene and the oxidation of the BDP derivative **2a** occur at a potential of ca. 600 mV vs Fc/Fc^+, it is not easy to distinguish which subunit of **2** is oxidized first (for the Br-BDP derivative **2a**, a reversible oxidation at $E_{1/2} = 630$ mV vs Fc/Fc^+ and a reversible reduction at $E_{1/2} = -1670$ mV vs Fc/Fc^+ were measured in CH_2Cl_2). For the monomer **2**, multicycle CVs scanning only over the first oxidation were sufficient to achieve electropolymerization. The CVs of the polymer film of **2** are dominated by a single oxidative wave at low oxidative potentials (Figure S-2, inset b), which is probably caused by oxidation of the BDP-substructure.

Electrochemical Polymerization of 3. The azulene-porphyrin dyad **3** also underwent electrochemical polymerization upon oxidation. Similar to compound **2**, two irreversible oxidative subwaves were found during the oxidation of the monomer.

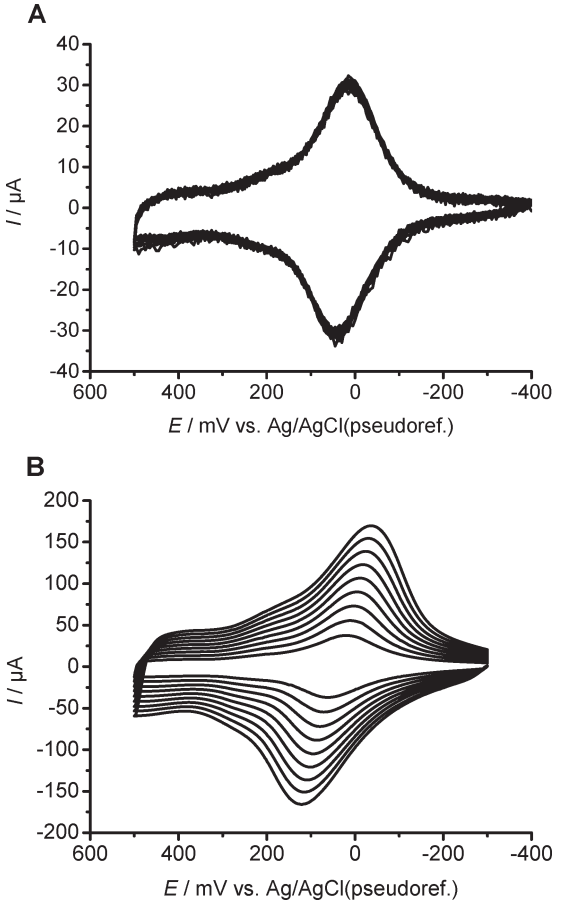

Figure 7. (A) Multicycle CVs of the polymer film of **1** in monomer free solution (CH_2Cl_2 + TBAH, 10 cycles) at a scan rate of 20 mV s^{-1}. (B) CVs of the polymer film of **1** in monomer free solution (CH_2Cl_2 + 0.2 M TBAH) at different scan rates (40−200 mV s^{-1}, smallest to largest cycle). The scan rate was increased in steps of 20 mV s^{-1}.

dx.doi.org/10.1021/jo200080v |J. Org. Chem. 2011, 76, 4859–4873

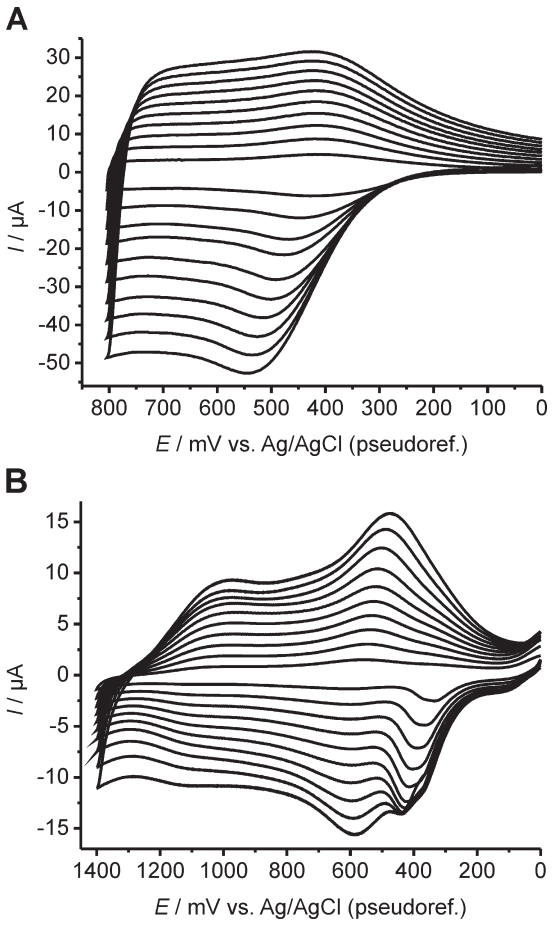

Figure 8. CVs of the polymer films of **3** (A) and **4** (B) in monomer-free solution (CH_2Cl_2 + 0.2 M TBAH) at different scan rates (20−200 mV s^{-1}, smallest to largest cycle). The scan rate was increased in steps of 20 mV s^{-1}.

The multicycle CVs for the potentiodynamic polymerization of **3** are depicted in Figure S-3. The anodic peak potential for the first oxidation of **3** is 530 mV vs Fc/Fc^+. The polymer films turned out to be stable, if charging-discharging steps were carried out up to moderately positive potentials (about 1 V vs Ag/AgCl pseudoref). The CVs of the polymer film of **3** in monomer-free solution (Figure 8A) look similar to those obtained for electrochemically polymerized azulene.[16]

Electrochemical Polymerization of 4. Finally, electrochemical polymerization of dyad **4** could also successfully be accomplished. The isoalloxazine substructure (in its quinone state) is not expected to undergo any further oxidation at positive potentials. The CVs showing the potentiodynamic polymerization of **4** are depicted in Figure S-4. The anodic oxidation peak in the initial cycle is at 670 mV vs Fc/Fc^+. As expected due to the electron withdrawing properties of the isoalloxazine substructure, this redox potential is slightly more positive than the potential of 600 mV vs Fc/Fc^+, which has been determined for the anodic oxidation of the parent azulene subunit.[16] Polymer films obtained by polymerization of **4** were stable and exhibited reversible electrochemical behavior upon moderate positive doping. The CVs of a polymer film of **4** in monomer-free solution collected at different scan rates are depicted in Figure 8B.

The potentials for the first anodic oxidation peak of **1**−**4** are summarized in Table 3. As expected, the first oxidation of the azulene-triarylamine dyad occurs at the lowest positive potential, whereas the oxidation of the azulene-isoalloxazine dyad requires the highest potential. Depending on the scan rate, the first oxidation of the dyads **1**−**4** results in the formation of polymers. Since the oxidation of all dyads is possible in a narrow potential range, it might be even possible to form mixed polymers by potentiodynamic copolymerization of **1**−**4** and bare azulene (E_{pa} = 600 mV vs Fc/Fc^+).

Table 3. Electrochemical Potential of the First Anodic Peak for Oxidation of the Azulene Dyads 1−4

	dyad			
	1	**2**	**3**	**4**
E_{pa} (mV) vs Fc/Fc^+	390	600	530	670

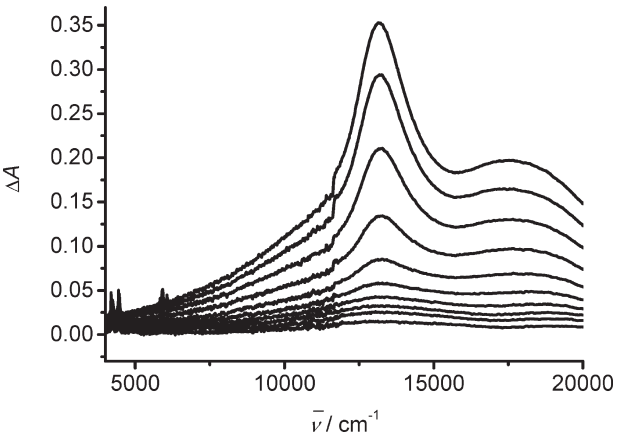

Figure 9. Spectroelectrochemistry of the polymer film of **1** in monomer-free solution (CH_2Cl_2 + 0.2 M TBAH) upon ongoing oxidation (doping). The potential was increased in steps of 50 mV. The signal at ca. 11500 cm^{-1} is an artifact of the instrument.

Spectroelectrochemistry. Representative spectroelectrochemical measurements were performed on the polymer films of **1** in reflection mode as depicted in Figure 9 (a Pt electrode served as mirror and as working electrode, differential spectra are shown). The charging and discharging of the film was performed over the potential region of the first oxidative subwave (Figure 7). A spectrum collected after the film was discharged again was identical to the initial spectrum (before charging and discharging), which confirmed the reversibility of the observed process. The spectra are dominated by the increase of a strong absorption band at 13,200 cm^{-1}, which is typical for triarylamine radical cations.[102,113−115] Besides this main absorption, a broad absorption in the low-energy region is present, which might be caused by intervalence charge transfer between neutral and positively charged triarylamines or triarylamine and azulene subunits. Hence, the triarylamine subunits have a strong influence on the optical and electrochemical properties of the polymer film. This might lead to improved hole conducting properties of the polymer film formed from **1** in comparison to pristine polyazulene.

CONCLUSION

In the present work, we have described a synthetic route for the preparation of 2-(4-ethynyl-phenyl)azulene (EPA) and have shown how EPA can be linked to halogenated dyes with different

dx.doi.org/10.1021/jo200080v |J. Org. Chem. 2011, 76, 4859–4873

optical and electrochemical properties by Pd-catalyzed cross-coupling reactions. The spectroscopic investigation of EPA has shown that fluorescence from the S_2 state is even possible for azulene derivatives possessing an energy gap between S_1 and S_2 state as small as 10,000 cm^{-1}. The chromophore-appended azulene dyads **1**−**4** exhibit strong absorption bands in the near-UV and visible range. Highly coplanar and π conjugated **1** shows strong charge-transfer interactions and is nonfluorescent. For **2** and **3**, irradiation in the visible leads to excitation of the appended BDP or porphyrin subchromophore, the fluorescence of which is partly quenched through energy transfer to azulene while possible charge-transfer interactions play only a minor role. For **4**, the quenching is even more pronounced, but the strong overlap of isoalloxazine S_1 and substituted azulene S_2 transitions precluded a more detailed analysis of the mechanism. The results reported here provide valuable insight into the features of dyads constructed from π extended azulene and chromophore units spanning the entire near-UV−vis absorption spectroscopic range. With respect to their use in OPV applications it should be kept in mind, however, that these optical properties are only valid for the monomeric azulene dyads, whereas polymers derived from them may differ.

Potentiodynamic oxidation of the dyads **1**−**4** led to the formation of polymer films, which were deposited at the electrode. As has been shown by spectroelectochemical investigations of the polymers of dyad **1**, a strong electronic interaction between the attached chromophore unit and the polyazulene backbone exists. Detailed investigations of the polymeric products are subject of future studies.

EXPERIMENTAL SECTION

Synthesis. *2-(4-Iodophenyl)-azulene-1-carbonitrile.* This reaction was carried out in darkness due to the light-sensitive starting material dihydroazulene (2-(4-iodophenyl)-2*H*-azulene-1,1-dicarbonitrile). Dihydroazulene (2.11 g, 5.52 mmol, M_r = 382.20, 1 equiv) was dissolved in 200 mL of abs CH_2Cl_2, and DBU (0.988 mL, 6.62 mmol, M_r = 152.24, d = 1.008 g/cm^3, 1.2 equiv) was added to this solution with continuous stirring. The reaction mixture was then stirred at room temperature, and the reaction was monitored by thin layer chromatography (TLC) (CH_2Cl_2/PE_{40-60} 2:1 ; R_f = 0.52). The product was identified as a violet spot on the TLC plate, whereas the starting material was found as a yellow spot that turned red when observed under light. After 2 days the reaction was complete. The solvent was removed on the rotary evaporator, and the remaining product was cleaned by column chromatography (SiO_2; CH_2Cl_2/PE 2:1, R_f = 0.5). The product was obtained as violet shiny crystals after crystallization from CH_2Cl_2/PE. Yield: 1.71 g, 3.04 mmol, 55%; mp = >189 °C; $C_{17}H_{10}NI$ 355.17 g/mol. Anal. Calcd: C 57.49, H 2.84, N 3.94. Found: C, 57.44, H 2.78, N 4.00. EI-MS (PI) M^+ 355 (100%), 356 (18%); (M − HI) 227 (94%), 228 (24%); additional peaks at 201 (33%), 200 (31%). ^{1}H NMR (400 MHz, $CDCl_3$): δ 8.66(1H, d, J = 9.67, H_8), 8.43(1H, d, J = 9.73, H_4), 7.87(2H, m, AA′, H_{10}), 7.84(1H, m, H_6), 7.81(2H, m, BB′, 2H, H_{11}), 7.56(1H, dd, H_7), 7.53(1H s, H_3), 7.52(1H, dd, H_5). ^{13}C NMR (100.6 MHz, $CDCl_3$): δ 150.8(C_9), 145.7(C_{8a}), 142.5(C_{3a}), 139.3(C_6), 138.4(C_{10}), 138.2(C_4), 136.1(C_8), 133.9(C_2), 130.2(C_{11}), 128.2(C_5), 128.0(C_7), 117.8(CN), 116.3(C_3), 95.9(C_{12}), 94.1(C_1). Determination was done by HSQC and HMBC; for atom numbering, see Chart S-1, Supporting Information.

2-(4-Iodophenyl)-azulene. 2-(4-Iodophenyl)-azulene-1-carbonitrile (0.806 g, 2.269 mmol, M_r = 355.17, 1 equiv) was dissolved in 12 mL of conc H_2SO_4. The yellow solution was stirred continuously while being heated to 100 °C in an oil bath. The reaction was monitored by TLC (CH_2Cl_2/PE_{40-60}; 2:1). After 1.5 h the reaction was complete. The reaction mixture was then added to 100 mL of ice−water, and the resulting light-blue suspension was neutralized with Na_2CO_3. The reaction mixture was then extracted from CH_2Cl_2 over 2 days on an extractor. The organic phase was collected, and the solvent was evaporated on the rotary evaporator. After evaporation, the bright shiny violet crystals were dried on the vacuum pump and dissolved in 30 mL of conc H_3PO_4 (85%). This yellow solution was stirred constantly while being heated to 100 °C, and the reaction was monitored by TLC (CH_2Cl_2/PE_{40-60}; 2:1). After 1 h the reaction was complete. The reaction mixture was then added to 100 mL of ice−water, which formed a blue precipitate. The suspension was then added to 100 mL of CH_2Cl_2 (the product dissolves partially in CH_2Cl_2), and the product was separated from the water phase 3 times with CH_2Cl_2 (or until the phase remaining in the separating funnel was colorless). The organic phases were collected together. After drying over Na_2SO_4, the solvent was removed on the rotary evaporator yielding a blue product. The product was then cleaned by column chromatography (SiO_2; solvent CH_2Cl_2; TLC control). The product containing fractions were combined, solvent was removed, and the product was dried on a vacuum pump. The product was obtained as blue shiny crystals that were crystallized from CH_2Cl_2/PE. Yield: 0.628 g, 1.90 mmol, 84%; mp = pyrolysis at 266−267 °C; $C_{16}H_{11}I$; 330.16 g/mol. Anal. Calcd: C, 58.21, H 3.36. Found: C, 58.06, H 3.41. EI-MS (PI) M^+: 330 (68%), 331 (13%). (M^+ − HI): 220 (100%) additional peaks at 176 (13%), 165 (19%). ^{1}H NMR (600 MHz, $CDCl_3$): δ 8.30(2H, d, $J_{4,5}$ = 9.2, H_4), 7.79 (2H, m, AA′, H_{11}), 7.69(2H, m, BB′, H_{10}), 7.64(2H, s, H_1), 7.54(1H, t, $J_{6,5}$ = 9.9, H_6), 7.17(2H, dd, $J_{4,5}$ = 9.2, $J_{6,5}$ = 9.9, H_5). ^{13}C NMR (150.9 MHz, $CDCl_3$): δ 148.5(C_2), 141.3(C_{3a}), 138.0(C_{11}), 136.9(C_6), 136.3(C_4), 136.0(C_9), 129.3(C_{10}), 124.0(C_5), 114.2(C_1), 94.0(C_{12}). Determination was done by HSQC and HMBC; for atom numbering, see Chart S-2, Supporting Information.

(4-Azulen-2-yl-phenylethynyl)-trimethyl-silane. 2-(4-Iodophenyl)-azulene (250 mg, 0.758 mmol), $PdCl_2(PPh_3)_2$ (16 mg, 23 μmol, 3 mol %) and CuI (2 mg, 0.011 mmol, 1.5 mol %) were dissolved in 5 mL of abs Et_3N under nitrogen atmosphere. Then trimethylsilylacetylene (118 μL, 0.834 mmol, 1.1 equiv) was added. The reaction mixture was stirred and heated to 55 °C for about 3 h (TLC control). The solvent was removed on the rotary evaporator. The product was then cleaned by column chromatography (SiO_2; solvent CH_2Cl_2; TLC control). The product containing fractions were combined, solvent was removed and the product was dried on a vacuum pump. Yield: 208 mg, 0.692 mmol, 91%; $C_{21}H_{20}Si$; 300.48 g/mol. ^{1}H NMR (600 MHz, $CDCl_3$): δ 8.28(2H, d, $J_{4,5}$ = 9.2, H_4), 7.90(2H, m, AA′, H_{10}), 7.66(2H, s, H_1), 7.55(2H, m, BB′, H_{11}), 7.52(1H, t, $J_{6,5}$ = 9.9, H_6), 7.16(2H, dd, $J_{4,5}$ = 9.2, $J_{6,5}$ = 9.9, H_5), 0.27(9H, s, $SiMe_3$). ^{13}C NMR (150.9 MHz, $CDCl_3$): δ 148.5(C_2), 141.2(C_{3a}), 136.5(C_6), 136.3(C_9), 136.0(C_4), 132.3(C_{11}), 127.1(C_{10}), 123.7(C_5), 122.5(C_{12}), 114.3(C_1), 105.0(C_{13}), 95.2(C_{14}), −0.3($SiMe_3$); δ-values taken of HMQC and HMBC from cross-coupling correlation; for atom numbering, see Chart S-3, Supporting Information.

2-(4-Ethynyl-phenyl)-azulene (EPA). (4-Azulen-2-yl-phenylethynyl)-trimethyl-silane (208 mg, 0.692 mmol) and 0.8 mL of 1 N KOH were dissolved in methanol (approximately 150 mL). The reaction mixture was stirred overnight at room temperature. The solvent was removed on the rotary evaporator, and the remaining product was cleaned by flash chromatography (SiO_2; preadsorption; solvent CH_2Cl_2/PE 1:1, R_f = 0.5). The product was obtained as violet shiny crystals after crystallization from CH_2Cl_2/PE. Yield: 98 mg, 0.429 mmol, 62%; mp = decomposition at 180 °C; $C_{18}H_{12}$; 228.29 g/mol. Anal. Calcd: C, 94.70, H 5.30. Found: C, 93.79, H 5.61. EI-MS (PI) M^+: 228 (100%), 229 (18%); M^{2+}: 114 (6%), additional peak at 226 (23%). ^{1}H NMR (600 MHz, $CDCl_3$): δ 8.29(2H, pd, $J_{4,5}$ = 10.1, H_4), 7.92 (2H, m, AA′, H_{10}), 7.66(2H, s, H_1), 7.58(2H, m, BB′, H_{11}), 7.53(1H, pt, $J_{6,5}$ = 10.0, H_6), 7.17(2H, dd, $J_{4,5}$ = 10.1, $J_{6,5}$ = 10.0, H_5), 3.17(1H, s, ethynyl). ^{13}C NMR (150.9 MHz, $CDCl_3$): δ 148.5(C_2), 141.1(C_{3a}), 136.66(C_9),

136.67(C_6), 136.2(C_4), 132.5(C_{11}), 127.2(C_{10}), 123.7(C_5), 121.5(C_{12}), 114.3(C_1), 83.5(C_{13}), 77.9(C_{14}); δ-values taken of HMQC and HMBC from cross-coupling correlation; for atom numbering, see Chart S-4, Supporting Information.

*[4-(4-Azulen-2-yl-phenylethynyl)-phenyl]-bis(4-methoxy-phenyl)-amine (**1**).* 2-(4-Ethynyl-phenyl)-azulene (40 mg, 0.175 mmol), *N*,*N*-Di(4-methoxyphenyl)-4-iodo-phenylamine[93] (86 mg, 0.2 mmol), $PdCl_2(PPh_3)_2$ (8 mg, 11 μmol, 7 mol %), and CuI (2 mg, 0.011 mmol, 7 mol %) were dissolved in 5 mL of abs Et_3N under nitrogen atmosphere. The reaction mixture was stirred at 55 °C for about 4 h. The solvent was removed, and the product was cleaned by flash chromatography (SiO_2; solvent CH_2Cl_2). The product containing fractions were combined, solvent was removed, and the product was dried in vacuo. Yield: 61 mg, 0.115 mmol, 66%; mp = 233−236 °C; $C_{38}H_{29}NO_2$; 531.65 g/mol. EI-MS (PI) M^+: 531 (100%), 532 (40%); M^{2+}: 265.5 (15%); additional peaks at: 516 (11%), 258 (11%). EI-MS (high resolution, PI): calcd 531.2198, found 531.2204; Δ = 1.1 ppm. ^{1}H NMR (600 MHz, $CDCl_3$): δ 8.28(d, $J_{4,5}$ = 9.3, 2H, C_4), 7.93 (m, AA′, 2H, Az-Ph), 7.68(s, 2H, C_1), 7.58(m, BB′, 2H, Az-Ph), 7.51(t, $J_{6,5}$ = 9.8, 1H, C_6), 7.33 (m, AA′, 2H, Am-Ph), 7.16(dd, $J_{4,5}$ = 9.3, $J_{6,5}$ = 9.8, 2H, C_5), 7.08(m, AA′, 4H, MeO-Ph), 6.87−6.84(m, BB′, Am-Ph, BB′, MeO-Ph, 6H), 3.81(s, 12H, MeO). ^{13}C NMR (150.9 MHz, $CDCl_3$): δ 156.2, 148.9, 148.7, 141.3, 140.1, 136.5, 136.0, 135.6, 132.3, 131.8, 127.3, 127.0, 123.7, 123.5, 119.0, 114.6, 114.3, 113.8, 91.3, 88.3, 55.4; δ-values taken of HMQC and HMBC from cross-coupling correlation.

2,6-Diethyl-1,3,5,7-tetramethyl-8-(p-bromophenyl)-4-difluorobor-3a,4a-diaza-(s)-indacene[94] *(**2a**).* *p*-Brombenzaldehyde (1.11 g, 6 mmol) and 3-ethyl-2,4-dimethylpyrrole (1.47 g, 12 mmol) were dissolved in 150 mL of abs CH_2Cl_2 under inert gas atmosphere. Three drops of trifluoroacetic acid were added. The reaction mixture was stirred for 4 h. Then, DDQ (1.36 g, 6 mmol) dissolved in CH_2Cl_2 was added and stirred for another 15 min. Subsequently, 6 mL of *N*-ethyl-diisopropylamine and 6 mL of $BF_3 \cdot Et_2O$ were added and stirred for 30 min. The reaction mixture was washed with water. The organic phase was dried over anhydrous $MgSO_4$. The solvent was evaporated. The product was purified by flash chromatography (SiO_2; preabsorption, petrolether/CH_2Cl_2, 8:1). The product was dissolved in a minimum amount of CH_2Cl_2 and crystallized by gradually adding *n*-hexane and evaporating the CH_2Cl_2. Fine green bright crystals were filtered off and dried in vacuo. Yield: 0.4 g, 0.87 mmol, 15%; mp = 266−259 °C; $C_{23}H_{26}BrN_2BF_2$; 459.19 g/mol. Anal. Calcd: C, 60.16, H 5.71, N 6.10. Found: C, 60.16, H 5.68, N 5.91. EI-MS (PI) M^+: 457 (26%), 458 (100%), 459 (50%), 460 (98%), 461 (24%); $M^+ - CH_3$: 442 (24%), 443 (98%), 444 (46%), 445 (97%), 446 (22%). ^{1}H NMR (400 MHz, $CDCl_3$): δ 7.63(2H, m, AA′), 7.18(2H, m, BB′), 2.53(6H, s, CH_3, C_3), 2.30(4H, q, J = 7.6 Hz), 1.32(6H, s, CH_3, C_1), 0.98(6H, t, J = 7.6 Hz). ^{13}C NMR (100.6 MHz, $CDCl_3$): δ 154.2, 138.5, 138.1, 134.8, 133.0, 132.3, 130.6, 130.2, 123.0, 17.0, 14.6, 12.5, 11.9.

*2,6-Diethyl-1,3,5,7-tetramethyl-8[4-(4-azulen-2-yl-phenyl-ethynyl)-phenyl]-4-difluorobor-3a,4a-diaza-(s)-indacene (**2**).* Br-BDP **2a** (63 mg, 0.137 mmol) and 2-(4-ethynyl-phenyl)-azulene (31 mg, 0.136 mmol) were dissolved in 2 mL of abs NEt_2 under inert gas atmosphere together with $Pd(PPh_3)_2Cl_2$ (6 mg, 11.4 μmol, 8.4 mol %) and CuI (1.5 mg, 7.88 μmol, 5.8 mol %). The reaction mixture was stirred for 4 h at 60 °C. The solvent was evaporated. The product was purified by flash chromatography (SiO_2, petrolether/CH_2Cl_2, 4:1). The product was dissolved in a minimum amount of CH_2Cl_2 and was crystallized by gradually adding *n*-hexane and evaporating the CH_2Cl_2. Fine red crystals were filtered off, washed with hexane, and dried in vacuo. Yield: 35 mg, 0.058 mmol, 43%; mp = >350 °C; $C_{41}H_{37}BF_2N_2$; 606.56 g/mol. Anal. Calcd: C, 81.19, H 6.16, N 4.62. Found: C, 81.19, H 6.06, N 4.41. EI-MS (PI) M^+: 607 (42%), 606 (100%), 605 (24%), M^{2+}: 303 (14%), additional peaks at: 592 (11%), 591 (29%), 296 (23%). ^{1}H NMR (600 MHz, $CDCl_3$): δ 8.31(2H, d, $J_{4,5}$ = 9.3, H_4), 7.98(2H, m, AA′, Az-Ph), 7.70(2H, s, H_1), 7.69(2H, m, AA′, Ph-BDP), 7.66(2H, m, BB′, Ph-Az), 7.54(1H. t, $J_{6,5}$ = 9.9 H_6), 7.31(2H, m, BB′, Ph-BDP), 7.18(2H, dd, $J_{4,5}$ = 9.3, $J_{6,5}$ = 9.9, H_5), 2.54(6H, s, CH_3, C_3), 2.31(4H, q, J = 7.6 Hz), 1.35(6H, s, CH_3, C_1), 0.99(6H, t, J = 7.6 Hz). ^{13}C NMR (150.9 MHz, $CDCl_3$): δ 154.0, 148.6, 141.3, 139.2, 138.2, 136.8, 136.6, 136.3, 135.7, 132.9, 132.1, 132.1, 130.5, 128.5, 127.5, 123.9, 123.9, 122.5, 114.4, 90.9, 89.9, 17.1, 14.5, 12.5, 11.9; δ-values taken of HMQC and HMBC from cross-coupling correlation.

5-(4-Bromo-phenyl)-10,15,20-tris(3,5-di-tert-butyl-phenyl)-porphyrin[95,96] *(**3a**).* To a mixture of 3,5-di-*tert*-butyl-benzaldehyde (1 g, 4.58 mmol), *p*-brombenzaldehyde (283 mg, 1.53 mmol), and $Zn(OAc)_2$ (0.336 g, 1.53 mmol) in propionic acid (100 mL) was added pyrrole (0.43 mL, 6.2 mmol) dissolved in propionic acid at 100 °C within 1 h under vigorous stirring. The resulting dark solution was refluxed for further 4 h and then cooled to room temperature. The solvent was evaporated, and the solid residue was purified by chromatography (short column, SiO_2, CH_2Cl_2). All product-containing fractions were collected. The volume was reduced to 100 mL, and pyridine (2 mL) and an excess of DDQ (2 g) were added at room temperature. The resulting mixture was stirred until the oxidation was complete (ca. 2 h). The cold solution was washed three times with 18% aqueous HCl solution (3 × 100 mL), neutralized with saturated aqueous $NaHCO_3$ solution (3 × 100 mL), washed with brine (1 × 100 mL), dried with Na_2SO_4, and evaporated to give a black-purple crude product. Purification by flash chromatography (SiO_2, petrolether/CH_2Cl_2: 8/1) yielded pure product as deep purple crystals. Yield: 0.095 g, 92.2 μmol, 6.0%; mp = >350 °C; $C_{68}H_{77}BrN_4$; 1030.29 g/mol. EI-MS (PI) M^+: 1032 (21%), 1031 (63%), 1030 (100%), 1029 (61%), 1028 (79%); M^{2+}: 515 (10%). ^{1}H NMR (400 MHz, $CDCl_3$): δ 8.91(4H, m, pyrrole), 8.91(2H, d, J = 4.77 Hz, pyrrole), 8.82(2H, d, J = 4.77 Hz, pyrrole), 8.11(2H, m, AA′), 8.09(4H, d, ABC system $\delta_A = \delta_B$, J = 1.83, H_{ortho}, 3,5-di-*tert*-butyl-phenyl at position 10 and 20), 8.08(2H, d, J = 1.86, H_{ortho}, 3,5-di-*tert*-butyl-phenyl at position 15), 7.89(2H, m, BB′), 7.81(2H t, ABC system $\delta_A = \delta_B$, J = 1.83, H_{para}, 3,5-di-*tert*-butyl-phenyl at position 10 and 20), 7.80(1H, t, J = 1.86, H_{para}, 3,5-di-*tert*-butyl-phenyl at position 15), 1.54(36H, s), 1.53(18H, s), −2.70(2H, s, NH).

*5-[4-(4-Azulen-2-yl-phenylethynyl)-phenyl]-10,15,20-tris(3,5-di-tert-butyl-phenyl)-porphyrin (**3**).* The porphyrin derivative **3a** (158 mg, 0.153 mmol) and 2-(4-ethynyl-phenyl)-azulene (35 mg, 0.153 mmol) were dissolved in abs NEt_3 (10 mL) under inert gas atmosphere together with $Pd_2(dba)_3CHCl_3$ (27 mg, 26 μmol), and CuI (2.5 mg, 13 μmol). Then tri-*tert*-butylphosphine (23 μL, 0.0773 mmol) was added and the reaction mixture was stirred at 55 °C overnight. The solvent was evaporated. The product was purified by flash chromatography (SiO_2; solvent CH_2Cl_2). The resulting red product was dried in vacuo after crystallization from PE/CH_2Cl_2. Yield: 82 mg, 70 μmol, 47%; mp = >350 °C; $C_{86}H_{88}N_4$; 1177.67 g/mol. EI-MS(PI) M^+: 1179(13%), 1178(38%), 1177(91%), 1176(100%); M^{2+}: 589.5(5%), 589(16%), 588.5(35%), 588(39%) EI-MS (high resolution, PI): calcd 1176.7009, found 1176.7032, Δ = 2.0 ppm. ^{1}H NMR (400 MHz, $CDCl_3$): δ 8.91(2H, d, J = 4.78 Hz, pyrrole, H_B), 8.90(4H, m, pyrrole), 8.87(2H, d, J = 4.78 Hz, pyrrole, H_A), 8.29(2H, d, J = 9.2 Hz, H_4-Az), 8.25(2H, m, AA′, H_{18}), 8.09(4H, d, ABC system $\delta_A = \delta_B$, J = 1.83, H_{ortho}, 3,5-di-*tert*-butyl-phenyl at position 10 and 20), 8.08(2H, d, J = 1.83, H_{ortho}, 3,5-di-*tert*-butyl-phenyl at position 15), 8.02(2H, m, AA′, H_{11}), 7.96(2H, m, BB′, H_{17}), 7.80(2H t, ABC system $\delta_A = \delta_B$, J = 1.83, H_{para}, 3,5-di-*tert*-butyl-phenyl at position 10 and 20), 7.79(1H, t, J = 1.83, H_{para}, 3,5-di-*tert*-butyl-phenyl at position 15), 7.77(2H, m, BB′, H_{12}), 7.71(2H, s, H_1-Az), 7.52(1H, t, J = 9.9 Hz, H_6-Az), 7.17(2H, pt, H_5-Az), 1.53(36H, s), 1.52(18H, s), −2.67(2H, s, NH). Determination was done by HSQC, HMBC and ROESY; for atom numbering, see Chart S-5, Supporting Information.

*10-(4-Bromo-phenyl)-3-heptyl-10H-benzo[g]pteridine-2,4-dione (**4a**).* A total of 100 mg (0.271 mmol, M_r = 369.174, 1 equiv) of 10-(4-bromo-phenyl)-10*H*-benzo[*g*]pteridine-2,4-dione (synthesized analogously to the corresponding Cl-derivative as described in ref 116), 0.449 mL (2.71 mmol, M_r = 226.102, d = 1.365, 10 equiv) of 1-iodoheptane, and

0.375 g (2.71 mmol, M_r = 138.204, 10 equiv) of K_2CO_3 were dissolved in abs DMF under nitrogen. The reaction was stirred at room temperature for 24 h in the dark. After the solvent was removed, the product was purified by chromatography. (SiO_2; CH_2Cl_2/MeOH 49:1). The product was obtained as yellow-green crystals after crystallization from CH_2Cl_2 and hexane. Yield: 66 mg; 0.141 mmol; 52%; mp = 319 °C, $C_{23}H_{23}BrN_4O_2$; 467.36 g/mol ESI-MS (PI) M^+: 467 (98%), 468 (27%), 469 (100%), 470 (26%). ^{1}H NMR ($CDCl_3$): δ 8.33(1H, m, H_6), 7.81(2H, m, AA′, ph), 7.68(1H, m, H_8), 7.60(1H, m, H_7), 7.22(2H, m, BB′, ph), 6.92(1H, m, H_9), 4.05(2H, t, J = 8.5, H_1), 1.68(2H, m, H_2), 1.27(8H, m, H_{3-6}), 0.87(3H, t, J = 6.8, H_7). ^{13}C NMR (100.6 MHz, $CDCl_3$): δ 159.1, 154.9, 149.8, 137.9, 135.6, 135.3, 134.2, 133.9, 133.8, 132.8, 129.3, 126.6, 124.8, 116.7, 42.2, 31.7, 29.0, 27.7, 26.9, 22.6, 14.1.

*10-[4-(4-Azulen-2-yl-phenylethynyl)-phenyl]-3-heptyl-10H-benzo-[g]pteridine-2,4-dione (**4**).* Compound **4a** (56 mg, 0.12 mmol) and 2-(4-ethynyl-phenyl)-azulene (27.7 mg, 0.12 mmol) were dissolved in abs NEt_3 (6 mL) under inert gas atmosphere together with $Pd_2(dba)_3CHCl_3$ (27 mg, 0.026 mmol) and CuI (3 mg, 0.016 mmol). Then tri-*tert*-butylphosphine (23 μL, 0.0773 mmol) was added, and the reaction mixture was stirred at 60 °C overnight. The solvent was evaporated. The product was purified by flash chromatography (Al_2O_3; solvent CH_2Cl_2). The solvent was removed, and the resulting olive-green product was dried in vacuo. Because the product still contained small traces of the starting material (Br-isoalloxazine derivative), further purification by HPLC was done before spectroscopic and electrochemical measurements were carried out. Yield: 30 mg, 0.049 mmol, 41%; mp = pyrolysis at 284 °C; $C_{41}H_{34}N_4O_2$; 614.75 g/mol. EI-MS(PI) M^+: 616(11%); 615(45%); 614(100%) EI-MS (high resolution, PI): calcd 616.2682, found 614.2670, Δ = 1.9 ppm. ^{1}H NMR (400 MHz, $CDCl_3$): δ 8.34(1H, m, H_6), 8.31(2H, d, J = 9.2 Hz, $H_{4,8}$-Az), 7.99(2H, m, AA′-ph-Az), 7.83(2H, m, AA′-ph-isoall.), 7.70(2H, s, $H_{1,3}$-Az), 7.69−7.66(3H, m, H_8 and BB′-ph-Az), 7.59(1H, m, H_7), 7.54(1H, t, J = 9.9 Hz, H_6-Az), 7.32(2H, m, B-ph-isoall.), 7.19(2H, m, $H_{5,7}$-Az), 6.94(1H, m, H_9), 4.08(2H, t, J = 7.4 Hz, CH_2 at C_1), 1.71(2H, m, CH_2 at C_2), 1.42−1.20(8H, m, 4 × CH_2 at C_{3-6}), 0.87(3H, t, J = 6.8 Hz, CH_3). ^{13}C NMR (100.6 MHz, $CDCl_3$): δ 159.2, 155.1, 149.9, 148.6, 141.4, 137.9, 136.94, 136.92, 136.5, 135.6, 135.3, 134.4, 133.9, 133.8, 132.8, 132.4, 127.8, 127.6, 126.5, 126.1, 124.0, 122.1, 116.8, 114.5, 92.1, 89.0, 42.2, 31.7, 29.0, 27.8, 26.9, 22.6, 14.1.

4-(4-Azulen-2-yl-phenylethynyl)-benzaldehyde. The synthesis was carried out from 2-(4-iodophenyl)-azulene and 4-ethynyl-benzaldehyde analogously to the synthesis of (4-azulen-2-yl-phenylethynyl)-trimethylsilane from 2-(4-iodophenyl)-azulene and trimethylsilylacetylene. Yield: 85%; $C_{25}H_{16}O$; 332.41 g/mol. ^{1}H NMR (600 MHz, $CDCl_3$): δ 9.96(s, 1H, $C_{aldehyde}$), 8.24(d, $J_{4,5}$ = 9.6 Hz, 2H, C_4), 7.91(m, AA′, 2H, Az-Ph), 7.82(m, AA′, 2H, COH-Ph), 7.63(m, BB′, 2H, COH-Ph), 7.62(s, 2H, C_1), 7.58(m, BB′, 2H, Az-Ph), 7.47(t, $J_{6,5}$ = 9.8, 1H, C_6), 7.12(pt, $J_{4,5}$ = $J_{6,5}$ = 9.7 Hz, 2H, C_5). ^{13}C NMR (150.9 MHz, $CDCl_3$): δ 191.4, 148.5, 141.4, 137.0, 136.9, 136.5, 135.4, 132.4, 132.1, 129.7, 129.6, 127.6, 124.0, 121.2, 114.5, 93.7, 89.7; δ-values taken of HMQC and HMBC from cross-coupling correlation.

*Azulene-fulleropyrrolidine dyad (**5**).* 4-(4-Azulen-2-yl-phenylethynyl)-benzaldehyde, *N*-isooctyl-glycine, and C_{60} were stirred in abs toluene under inert gas atmosphere at 90−100 °C overnight. Thereafter the volume of the solvent was decreased under reduced pressure. Upon filtration, a dark-brown solid remained that was washed three times with CH_2Cl_2. The crude product was only soluble in very low concentration in toluene and CS_2. Moreover, it exhibited rather poor solubility in common organic solvents. Therefore, further purification by chromatography was not possible. $C_{94}H_{35}N$; 1178.32 g/mol. The product was identified by mass spectroscopy: ESI-MS (PI) MH^+: 1178.5 (98%), 1179.5 (100%), 1180.5 (65%), 1181.5 (30%). A ^{1}H NMR spectrum (CS_2/$CDCl_3$ ca. 9/1) showed peaks between 8.5 and 4 ppm that are characteristic for the azulene and the fulleropyrrolidine substructure.

Steady-State Absorption and Fluorescence Spectroscopy. Steady-state absorption and fluorescence measurements were carried out on a UV−vis−NIR spectrophotometer and a traceably characterized spectrofluorometer.[117,118] For all room temperature measurements, the temperature was kept constant at 298 ± 1 K. Unless otherwise noted, only dilute solutions with an absorbance of less than 0.1 at the absorption maximum were used. Fluorescence experiments were performed with a 90° standard geometry, with polarizers set at 54.7° for emission and 0° for excitation. The fluorescence quantum yields (Φ_f) were determined relative to coumarin 102 in ethanol (excitation range <400 nm, Φ_f = 0.765 ± 0.004)[117] coumarin 153 in ethanol (excitation range 400−440 nm, Φ_f = 0.542 ± 0.005),[117] 4-dicyanomethylene-2-methyl-6-(*p*-dimethylaminostyryl)-4*H*-pyran (DCM) in ethanol (excitation range 440−480 nm, Φ_f = 0.433 ± 0.004),[117] and **12** in MeCN (excitation range 480−520 nm, Φ_f = 0.87 ± 0.02),[63] respectively. The uncertainties of measurement were determined to ±5% (for Φ_f > 0.2), ± 10% (for 0.2 > Φ_f > 0.02) and ±20% (for 0.02 > Φ_f). For the experiments involving **2**−**4**, excitation wavelengths were chosen in a region in which almost exclusively the appended chromophore absorbed and absorption of the π-extended azulene fragment was negligible, i.e., ca. 430−480 nm. The low-temperature measurements were performed with a continuous flow cryostat. Liquid nitrogen was pumped from a storage container via a transfer tube by a gas flow pump through the cryostat. The temperature was externally controlled. The temperature in the sample rod was monitored via the temperature-dependent resistance of a sensor that was calibrated with a Peltier element.

Time-Resolved Fluorescence Spectroscopy. Fluorescence lifetimes (τ_f) were determined by a unique customized laser impulse fluorometer with picosecond time resolution, which we have described in earlier publications.[119,120] The fluorescence was collected at right angles (polarizer set at 54.7°; monochromator with spectral bandwidths of 4, 8, and 16 nm), and the fluorescence decays were recorded with a modular single photon timing unit described in ref 120. While realizing typical instrumental response functions of fwhm of ca. 25−30 ps, the time division was 4.8 ps channel^{-1} and the experimental accuracy amounted to ±3 ps, respectively. The laser beam was attenuated using a double prism attenuator and typical excitation energies were in the nanowatt to microwatt range (average laser power). The fluorescence lifetime profiles were analyzed with a PC using the software package Global Unlimited V2.2 (Laboratory for Fluorescence Dynamics, University of Illinois). The goodness of the fit of the single decays as judged by reduced chi-squared (χ_R^2) and the autocorrelation function C(j) of the residuals was always below χ_R^2 < 1.2.

Computational Details. The optimization of the S_0 ground state geometries in the gas phase was performed with the density functional theory (DFT) method employing the hybrid functional B3LYP with a 6-31G basis set and energy-minimized as implemented in Gaussian 03.[121]

Electrochemical Setup. Cyclic voltammetry measurements were performed at room temperature using an undivided electrochemical cell with a three-electrode arrangement and a computer-controlled potentiostat/galvanostat. As working electrode, we used a homemade platinum disk electrode together with an Ag/AgCl pseudoreference- and a platinum counter electrode. As supporting electrolyte, tetrabutyl-ammonium hexafluoro-phosphate (TBAH) was used. For electrochemical experiments 5 mg of the compounds were dissolved in 5−8 mL of the solvent. Spectroelectrochemistry was measured in reflection at a homemade platinum disk electrode.

■ ASSOCIATED CONTENT

Supporting Information. Synthesis of DHA, synthesis of **5**, supplementary figures for electrochemical polymerization results, atom numbering for NMR results in Experimental

Section, and copies of NMR spectra. This material is available free of charge via the Internet at http://pubs.acs.org.

AUTHOR INFORMATION

Corresponding Author
*E-mail: noell@chemie.uni-siegen.de; knut.rurack@bam.de.

ACKNOWLEDGMENT

This work was supported by the DFG (GRK 640 "Sensory Photoreceptors in Natural and Artificial Systems") and country North Rhine-Westphalia. K.R. thanks M. Spieles and D. Gröninger (Div. 1.5, BAM) for experimental support.

REFERENCES

(1) *Organic Photovoltaics, Mechanisms, Materials, and Devices*; Sun, S.-S., Sariciftci, N. S., Eds.; Taylor & Francis: Boca Raton, FL, 2005.
(2) Hoppe, H.; Sariciftci, N. S. *J. Mater. Chem.* **2006**, *16*, 45–61.
(3) Segura, J. L.; Martin, N.; Guldi, D. M. *Chem. Soc. Rev.* **2005**, *34*, 31–47.
(4) Roncali, J. *Chem. Soc. Rev.* **2005**, *34*, 483–495.
(5) Bäuerle, P.; Cremer, J. *Chem. Mater.* **2008**, *20*, 2696–2703.
(6) Cremer, J.; Bäuerle, P.; Wienk, M. M.; Janssen, R. A. J. *Chem. Mater.* **2006**, *18*, 5832–5834.
(7) Scharber, M. C.; Mühlbacher, D.; Koppe, M.; Denk, P.; Waldauf, C.; Heeger, A. J.; Brabec, C. J. *Adv. Mater.* **2006**, *18*, 789–794.
(8) Ma, C.-Q.; Mena-Osteritz, E.; Debaerdemaeker, T.; Wienk, M. M.; Janssen, R. A. J.; Bäuerle, P. *Angew. Chem., Int. Ed.* **2007**, *46*, 1679–1683.
(9) Dastoor, P. C.; McNeill, C. R.; Frohne, H.; Foster, C. J.; Dean, B.; Fell, C. J.; Belcher, W. J.; Campbell, W. M.; Officer, D. L.; Blake, I. M.; Thordarson, P.; Crossley, M. J.; Hush, N. S.; Reimers, J. R. *J. Phys. Chem. C* **2007**, *111*, 15415–15426.
(10) Burke, A.; Ito, S.; Snaith, H.; Bach, U.; Kwiatkowski, J.; Grätzel, M. *Nano Lett.* **2008**, *8*, 977–981.
(11) Walzer, K.; Männig, B.; Pfeiffer, M.; Leo, K. *Chem. Rev.* **2007**, *107*, 1233–1271.
(12) Lo, S.-C.; Burn, P. L. *Chem. Rev.* **2007**, *107*, 1097–1116.
(13) Roncali, J.; Leriche, P.; Cravino, A. *Adv. Mater.* **2007**, *19*, 2045–2060.
(14) Brauer, J. C.; Thorsmolle, V. K.; Moser, J.-E. *Chimia* **2009**, *63*, 189–192.
(15) Heinze, J.; Frontana-Uribe, B. A.; Ludwigs, S. *Chem. Rev.* **2010**, *110*, 4724–4771.
(16) Nöll, G.; Lambert, C.; Lynch, M.; Porsch, M.; Daub, J. *J. Phys. Chem. C* **2008**, *112*, 2156–2164.
(17) Tanabe, J.; Shinkai, M.; Tsuchiya, M. Durable azulene dyes, electrodes therefrom, and photoelectric converters therewith. Patent JP2008101065, 2008.
(18) Schulte, N.; Scheurich, R. P.; Pan, J. Conjugated polymers and dendrimers, process for their preparation and their use. Patent WO2008019744, 2008.
(19) O'Regan, B. C.; Lopez-Duarte, I.; Martinez-Diaz, M. V.; Forneli, A.; Albero, J.; Morandeira, A.; Palomares, E.; Torres, T.; Durrant, J. R. *J. Am. Chem. Soc.* **2008**, *130*, 2906–2907.
(20) Zhang, X.-H.; Li, C.; Wang, W.-B.; Cheng, X.-X.; Wang, X.-S.; Zhang, B.-W. *J. Mater. Chem.* **2007**, *17*, 642–649.
(21) Buvat, P.; Odobel, F.; Houarnier, C.; Blart, E. Sensitizing compositions for solar cells with semiconducting ceramic oxides grafted functionally to polymeric conductors and ruthenium complexes. Patent WO2007071792, 2007.
(22) Farrand, L.; Findlater, M.; Giles, M.; Heeney, M.; Tierney, S.; Thompson, M.; Shkunov, M.; Sparrowe, D.; McCulloch, I. Mono-, oligo- and polymers comprising a 2,6-azulene group and their use as charge transport materials. Patent EP1318183, 2003.
(23) Farrand, L.; Findlater, M.; Giles, M.; Heeney, M.; Tierney, S.; Thompson, M.; Shkunov, M.; Sparrowe, D.; McCulloch, I. Reactive mesogenic azulenes. Patent EP1318185, 2003.
(24) Gui, J. Y.; Spivack, J. L.; Duggal, A. R.; Cella, J. A.; Alizadeh, A.; Yakimov, A. Molecular photovoltaics, method of manufacture and articles derived therefrom. Patent US2006021647, 2006.
(25) Lamberto, M.; Pagba, C.; Piotrowiak, P.; Galoppini, E. *Tetrahedron Lett.* **2005**, *46*, 4895–4899.
(26) Pagba, C.; Zordan, G.; Galoppini, E.; Piatnitski, E. L.; Hore, S.; Deshayes, K.; Piotrowiak, P. *J. Am. Chem. Soc.* **2004**, *126*, 9888–9889.
(27) Zhang, Y.; Galoppini, E. *ChemSusChem* **2010**, *3*, 410–428.
(28) Bagala Rampazzo, L.; Matiello, L. Carbonyl derivatives having a C3 symmetry, their preparation and uses thereof. Patent WO2010038252, 2010.
(29) Ono, Y.; Kawanabe, T.; Aodeng, G. Method of manufacturing polymer thin film. Patent JP2009155437, 2009.
(30) Ono, Y.; Shinohara, T. Manufacturing method of dye-sensitized solar cell. Patent JP2009059499, 2009.
(31) Mirlach, A.; Feuerer, M.; Daub, J. *Adv. Mater.* **1993**, *5*, 450–453.
(32) Latonen, R.-M.; Kvarnstroem, C.; Ivaska, A. *J. Appl. Electrochem.* **2010**, *40*, 1583–1591.
(33) Wang, F.; Lai, Y.-H.; Kocherginsky, N. M.; Koteski, Y. Y. *Org. Lett.* **2003**, *5*, 995–998.
(34) Waltman, R. J.; Bargon, J. *Can. J. Chem.* **1986**, *64*, 76–95.
(35) Nie, G.; Cai, T.; Zhang, S.; Hou, J.; Xu, J.; Han, X. *Mater. Lett.* **2007**, *61*, 3079–3082.
(36) Meana-Esteban, B.; Lete, C.; Kvarnstroem, C.; Ivaska, A. *J. Phys. Chem. B* **2006**, *110*, 23343–23350.
(37) Porsch, M.; Sigl-Seifert, G.; Daub, J. *Adv. Mater.* **1997**, *9*, 635–639.
(38) Redl, F. X.; Köthe, O.; Röckl, K.; Bauer, W.; Daub, J. *Macromol. Chem. Phys.* **2000**, *201*, 2091–2100.
(39) Schuhmann, W.; Huber, J.; Mirlach, A.; Daub, J. *Adv. Mater.* **1993**, *5*, 124–126.
(40) Mirlach, A.; Salbeck, J.; Daub, J. *DECHEMA Monogr.* **1989**, *117*, 367–381.
(41) Daub, J.; Feuerer, M.; Mirlach, A.; Salbeck, J. *Synth. Met.* **1991**, *42*, 1551–1555.
(42) Mrozek, T.; Daub, J.; Ajayaghosh, A. In *Molecular Switches*; Feringa, B. L., Ed.; Wiley-VCH: Weinheim, Germany, 2001; pp 63−106.
(43) Bross, P. A.; Mirlach, A.; Salbeck, J.; Daub, J. *DECHEMA Monogr.* **1990**, *121*, 375–382.
(44) As an additional combination of azulene with a strong electron acceptor and because fullerene derivatives are currently one of the most promising electron acceptors for organic photovoltaic applications, an azulene-fullerene dyad **5** (see Section II, Supporting Information and Experimental Section) was also targeted.
(45) Lloyd, M. T.; Anthony, J. E.; Malliaras, G. G. *Mater. Today* **2007**, *10*, 34–41.
(46) Shirota, Y.; Kageyama, H. *Chem. Rev.* **2007**, *107*, 953–1010.
(47) Pai, D. M.; Yanus, J. F.; Stolka, M. *J. Phys. Chem.* **1984**, *88*, 4714–4717.
(48) Stolka, M.; Yanus, J. F.; Pai, D. M. *J. Phys. Chem.* **1984**, *88*, 4707–4714.
(49) Shirota, Y. *J. Mater. Chem.* **2005**, *15*, 75–93.
(50) Shirota, Y. *J. Mater. Chem.* **2000**, *10*, 1–25.
(51) Grätzel, M. In *Electron Transfer in Chemistry*; Balzani, V., Ed.; Wiley-VCH: Weinheim, 2001; Vol. 5, pp 589−644.
(52) West, D. P.; Rahn, M. D. In *Electron Transfer in Chemistry*; Balzani, V., Ed.; Wiley-VCH: Weinheim, 2001; Vol. 5, p 472−515.
(53) Pålsson, L. O.; Wang, C.; Batsanov, A. S.; King, S. M.; Beeby, A.; Monkman, A. P.; Bryce, M. R. *Chem.—Eur. J.* **2010**, *16*, 1470–1479.
(54) Ando, Y.; Iino, S.; Yamada, K.; Umezawa, K.; Iwasawa, N.; Citterio, D.; Suzuki, K. *Sens. Actuators, B* **2007**, *B121*, 74–82.
(55) Röhr, H.; Trieflinger, C.; Rurack, K.; Daub, J. *Chem.—Eur. J.* **2006**, *12*, 689–700.
(56) Kollmannsberger, M.; Rurack, K.; Resch-Genger, U.; Rettig, W.; Daub, J. *Chem. Phys. Lett.* **2000**, *329*, 363–369.

(57) Yuan, M.; Li, Y.; Li, J.; Li, C.; Liu, X.; Lv, J.; Xu, J.; Liu, H.; Wang, S.; Zhu, D. *Org. Lett.* **2007**, *9*, 2313–2316.
(58) Destandau, E.; Lefevre, J.-P.; Chouai Fakhr Eddine, A.; Desportes, S.; Jullien, M. C.; Hierle, R.; Leray, I.; Valeur, B.; Delaire, J. A. *Anal. Bioanal. Chem.* **2007**, *387*, 2627–2632.
(59) Yogo, T.; Urano, Y.; Ishitsuka, Y.; Maniwa, F.; Nagano, T. *J. Am. Chem. Soc.* **2005**, *127*, 12162–12163.
(60) Ozlem, S.; Akkaya, E. U. *J. Am. Chem. Soc.* **2009**, *131*, 48–49.
(61) Lim, S. H.; Thivierge, C.; Nowak-Sliwinska, P.; Han, J.; van den Bergh, H.; Wagnieres, G.; Burgess, K.; Lee, H. B. *J. Med. Chem.* **2010**, *53*, 2865–2874.
(62) Trieflinger, C.; Rurack, K.; Daub, J. *Angew. Chem., Int. Ed.* **2005**, *44*, 2288–2291.
(63) Trieflinger, C.; Röhr, H.; Rurack, K.; Daub, J. *Angew. Chem., Int. Ed.* **2005**, *44*, 6943–6947.
(64) Xiao, S.; Zou, Y.; Wu, J.; Zhou, Y.; Yi, T.; Li, F.; Huang, C. *J. Mater. Chem.* **2007**, *17*, 2483–2489.
(65) Tomasulo, M.; Deniz, E.; Alvarado, R. J.; Raymo, F. M. *J. Phys. Chem. C* **2008**, *112*, 8038–8045.
(66) Bailey, S. T.; Lokey, G. E.; Hanes, M. S.; Shearer, J. D. M.; McLafferty, J. B.; Beaumont, G. T.; Baseler, T. T.; Layhue, J. M.; Broussard, D. R.; Zhang, Y.-Z.; Wittmershaus, B. P. *Sol. Energy Mater. Sol. Cells* **2007**, *91*, 67–75.
(67) Ziessel, R.; Goze, C.; Ulrich, G.; Cesario, M.; Retailleau, P.; Harriman, A.; Rostron, J. P. *Chem.—Eur. J.* **2005**, *11*, 7366–7378.
(68) Harriman, A.; Mallon, L. J.; Elliot, K. J.; Haefele, A.; Ulrich, G.; Ziessel, R. *J. Am. Chem. Soc.* **2009**, *131*, 13375–13386.
(69) Koepf, M.; Trabolsi, A.; Elhabiri, M.; Wytko, J. A.; Paul, D.; Albrecht-Gary, A. M.; Weiss, J. *Org. Lett.* **2005**, *7*, 1279–1282.
(70) Meng, G.; Velayudham, S.; Smith, A.; Luck, R.; Liu, H. *Macromolecules* **2009**, *42*, 1995–2001.
(71) Alemdaroglu, F. E.; Alexander, S. C.; Ji, D.; Prusty, D. K.; Borsch, M.; Herrmann, A. *Macromolecules* **2009**, *42*, 6529–6536.
(72) Imahori, H.; Norieda, H.; Yamada, H.; Nishimura, Y.; Yamazaki, I.; Sakata, Y.; Fukuzumi, S. *J. Am. Chem. Soc.* **2001**, *123*, 100–110.
(73) Liu, J.-Y.; Yeung, H.-S.; Xu, W.; Li, X.; Ng, D. K. P. *Org. Lett.* **2008**, *10*, 5421–5424.
(74) Terazono, Y.; Kodis, G.; Liddell, P. A.; Garg, V.; Moore, T. A.; Moore, A. L.; Gust, D. *J. Phys. Chem. B* **2009**, *113*, 7147–7155.
(75) Kamat, P. V. *J. Phys. Chem. C* **2007**, *111*, 2834–2860.
(76) Yamada, H.; Imahori, H.; Nishimura, Y.; Yamazaki, I.; Ahn, T. K.; Kim, S. K.; Kim, D.; Fukuzumi, S. *J. Am. Chem. Soc.* **2003**, *125*, 9129–9139.
(77) Kurotobi, K.; Osuka, A. *Org. Lett.* **2005**, *7*, 1055–1058.
(78) Yeow, E. K. L.; Ziolek, M.; Karolczak, J.; Shevyakov, S. V.; Asato, A. E.; Maciejewski, A.; Steer, R. P. *J. Phys. Chem. A* **2004**, *108*, 10980–10988.
(79) Kurotobi, K.; Kim, K. S.; Noh, S. B.; Kim, D.; Osuka, A. *Angew. Chem., Int. Ed.* **2006**, *45*, 3944–3947.
(80) Kim, K. S.; Noh, S. B.; Katsuda, T.; Ito, S.; Osuka, A.; Kim, D. *Chem. Commun* **2007**, 2479–2481.
(81) *Handbook of Photosensory Receptors*; Briggs, W. R., Spudich, J., L, Eds.; Wiley-VCH: Weinheim, Germany, 2005.
(82) Briggs, W. R. *Compr. Ser. Photochem. Photobiol. Sci.* **2006**, *6*, 183–216.
(83) Ahmad, M. In *Handbook of Photochemistry and Photobiology*; Nalwa, H. S., Ed.; American Scientific Publishers: Valencia, CA, 2003; Vol. 4, pp 159−182.
(84) Behrens, C.; Cichon, M. K.; Grolle, F.; Hennecke, U.; Carell, T. *Top. Curr. Chem.* **2004**, *236*, 187–204.
(85) Cravino, A.; Sariciftci, N. S. *J. Mater. Chem.* **2002**, *12*, 1931–1943.
(86) Cravino, A. *Polym. Int.* **2007**, *56*, 943–956.
(87) Gobbi, L.; Seiler, P.; Diederich, F.; Gramlich, V.; Boudon, C.; Gisselbrecht, J.-P.; Gross, M. *Helv. Chim. Acta* **2001**, *84*, 743–777.
(88) Gierisch, S.; Daub, J. *Chem. Ber.* **1989**, *122*, 69–75.
(89) Nozoe, T.; Takase, K.; Fukuda, S. *Bull. Chem. Soc. Jpn.* **1971**, *44*, 2210–2213.
(90) Bindl, J.; Daub, J.; Hasenhündl, A.; Meinert, M.; Rapp, K. M. *Chem. Ber.* **1983**, *116*, 2408–2417.
(91) Baier, M.; Daub, J.; Hasenhündl, A.; Merz, A.; Rapp, K. M. *Angew. Chem., Int. Ed.* **1981**, *20*, 198–199.
(92) Petersen, M. A.; Kilsaa, K.; Kadziola, A.; Nielsen, M. B. *Eur. J. Org. Chem.* **2007**, 1415–1418.
(93) Lambert, C.; Nöll, G.; Schmalzlin, E.; Meerholz, K.; Bräuchle, C. *Chem.—Eur. J.* **1998**, *4*, 2129–2135.
(94) Benniston, A. C.; Copley, G.; Elliott, K. J.; Harrington, R. W.; Clegg, W. *Eur. J. Org. Chem.* **2008**, 2705–2713.
(95) Beavington, R.; Burn, P. L. *J. Chem. Soc., Perkin Trans. 1* **1999**, 583–592.
(96) Hammel, D.; Kautz, C.; Müllen, K. *Chem. Ber.* **1990**, *123*, 1353–6.
(97) Rudzki Small, J.; Hutchings, J. J.; Small, E. W. *Proc. SPIE-Int. Soc. Opt. Eng.* **1989**, *1054*, 26–35.
(98) Wagner, B. D.; Tittelbach-Helmrich, D.; Steer, R. P. *J. Phys. Chem.* **1992**, *96*, 7904–7908.
(99) Yamaguchi, H.; Sato, S.; Yasunam, M.; Sato, T.; Yoshinobu, M. *Spectrochim. Acta, Part A* **1997**, *53A*, 2471–2473.
(100) Tetreault, N.; Muthyala, R. S.; Liu, R. S. H.; Steer, R. P. *J. Phys. Chem. A* **1999**, *103*, 2524–2531.
(101) Amthor, S.; Lambert, C.; Dümmler, S.; Fischer, I.; Schelter, J. *J. Phys. Chem. A* **2006**, *110*, 5204–5214.
(102) Nöll, G.; Avola, M.; Lynch, M.; Daub, J. *J. Phys. Chem. C* **2007**, *111*, 3197–3204.
(103) Lambert, C.; Schelter, J.; Fiebig, T.; Mank, D.; Trifonov, A. *J. Am. Chem. Soc.* **2005**, *127*, 10600–10610.
(104) Shizuka, H.; Takayama, Y.; Tanaka, I.; Morita, T. *J. Am. Chem. Soc.* **1970**, *92*, 7270–7277.
(105) Lambert, C.; Nöll, G.; Zabel, M.; Hampel, F.; Schmälzlin, E.; Bräuchle, C.; Meerholz, K. *Chem.—Eur. J.* **2003**, *9*, 4232–4239.
(106) Note that 2-(4-(phenylethynyl)phenyl)azulene was not available as a model compound and would presumably show somewhat changed features as EPA. Modelling of the spectrum of **2** from the spectra of EPA and the parent BDP chromophore was thus not attempted.
(107) Wu, P.; Brand, L. *Anal. Biochem.* **1994**, *218*, 1–13.
(108) Excitation below 420 nm also gave rise to the typical porphyrin fluorescence but did not yield measurable traces of EPA S_2 fluorescence.
(109) Zhang, X. H.; Xie, Z. Y.; Wu, F. P.; Zhou, L. L.; Wong, O. Y.; Lee, C. S.; Kwong, H. L.; Lee, S. T.; Wu, S. K. *Chem. Phys. Lett.* **2003**, *382*, 561–566.
(110) Because **3a** had to be employed as reference compound for the lifetime (determined to 5.17 ns) and the fluorescence quantum yield (determined to 0.08) of the unperturbed donor and because **3** showed traces of decomposition during the fluorescence lifetime measurements, the uncertainty of these data is larger than in the case of **2**.
(111) Note that the solubility of **4** was too low in Bu_2O to yield reliable data.
(112) Amthor, S.; Noller, B.; Lambert, C. *Chem. Phys.* **2005**, *316*, 141–152.
(113) Nöll, G.; Amthor, S.; Avola, M.; Lambert, C.; Daub, J. *J. Phys. Chem. C* **2007**, *111*, 3512–3516.
(114) Lambert, C.; Nöll, G. *J. Chem. Soc., Perkin Trans. 2* **2002**, 2039–2043.
(115) Lambert, C.; Nöll, G. *J. Am. Chem. Soc.* **1999**, *121*, 8434–8442.
(116) Kirsch, P.; Schoenleben-Janas, A.; Schirmer, R. H. *Liebigs Ann. Chem.* **1995**, 1275–1281.
(117) Rurack, K.; Spieles, M. *Anal. Chem.* **2011**, *83*, 1232–1242.
(118) Resch-Genger, U.; Pfeifer, D.; Monte, C.; Pilz, W.; Hoffmann, A.; Spieles, M.; Rurack, K.; Hollandt, J.; Taubert, T.; Schönenberger, B.; Nording, P. *J. Fluoresc.* **2005**, *15*, 315–336.
(119) Resch, U.; Rurack, K. *Proc. SPIE-Int. Soc. Opt. Eng.* **1997**, *3105*, 96–103.
(120) Shen, Z.; Röhr, H.; Rurack, K.; Uno, H.; Spieles, M.; Schulz, B.; Reck, G.; Ono, N. *Chem.—Eur. J.* **2004**, *10*, 4853–4871.
(121) Frisch, M. J.; Trucks, G. W.; Schlegel, H. B.; Scuseria, G. E.; Robb, M. A.; Cheeseman, J. R.; Montgomery, J. A.; Vreven, T.; Kudin, K. N.; Burant, J. C.; Millam, J. M.; Iyengar, S. S.; Tomasi, J.; Barone, V.; Mennucci, B.; Cossi, M.; Scalmani, G.; Rega, N.; Petersson,

G. A.; Nakatsuji, H.; Hada, M.; Ehara, M.; Toyota, K.; Fukuda, R.; Hasegawa, J.; Ishida, M.; Nakajima, T.; Honda, Y.; Kitao, O.; Nakai, H.; Klene, M.; Li, X.; Knox, J. E.; Hratchian, H. P.; Cross, J. B.; Adamo, C.; Jaramillo, J.; Gomperts, R.; Stratmann, R. E.; Yazyev, O.; Austin, A. J.; Cammi, R.; Pomelli, C.; Ochterski, J. W.; Ayala, P. Y.; Morokuma, K.; Voth, G. A.; Salvador, P.; Dannenberg, J. J.; Zakrzewski, V. G.; Dapprich, S.; Daniels, A. D.; Strain, M. C.; Farkas, O.; Malick, D. K.; Rabuck, A. D.; Raghavachari, K.; Foresman, J. B.; Ortiz, J. V.; Cui, Q.; Baboul, A. G.; Clifford, S.; Cioslowski, J.; Stefanov, B. B.; Liu, G.; Liashenko, A.; Piskorz, P.; Komaromi, I.; Martin, R. L.; Fox, D. J.; Keith, T.; Al-Laham, M. A.; Peng, C. Y.; Nanayakkara, A.; Challacombe, M.; Gill, P. M. W.; Johnson, B.; Chen, W.; Wong, M. W.; Gonzalez, C.; Pople, J. A. *Gaussian 03, revision D.01*; Gaussian, Inc.: Wallingford, CT, 2004.